

Weakly dynamic dark energy via metric-scalar couplings with torsion

Sourav Sur* and Arshdeep Singh Bhatia†

*Department of Physics & Astrophysics
University of Delhi, New Delhi - 110 007, India*

Abstract

We study the dynamical aspects of dark energy in the context of a non-minimally coupled scalar field with curvature and torsion. Whereas the scalar field acts as the source of the trace mode of torsion, a suitable constraint on the pseudo-trace of the latter provides a mass term for the scalar field in the effective action. In the equivalent scalar-tensor framework, we find explicit cosmological solutions suitable for describing dark energy in both Einstein and Jordan frames. We demand the dynamical evolution of the dark energy to be weak enough, so that the present-day values of the cosmological parameters could be estimated keeping them within the confidence limits set for the standard Λ CDM model from recent observations. For such estimates, we examine the variations of the effective matter density and the dark energy equation of state over different redshift ranges. In spite of being weakly dynamic, the dark energy component here differs significantly from the cosmological constant, both in characteristics and features, for e.g. it interacts with the cosmological (dust) fluid in the Einstein frame, and crosses the phantom barrier in the Jordan frame. We also obtain the upper bounds on the torsion mode parameters and the lower bound on the effective Brans-Dicke parameter. The latter turns out to be fairly large, and in agreement with the local gravity constraints, which therefore come in support of our analysis.

PACS numbers: xxxxxxxx

1 Introduction

Despite a host of recent developments, cosmology is faced with a vexed question: *to what extent a dynamical evolution of dark energy (DE) is tenable, as opposed to a cosmological constant Λ , in driving the late-time cosmic acceleration?* [1, 2]. While the theoretical motivation for the DE dynamics is evident from the well-known “fine tuning” problem with Λ [3], observations grossly favour the Λ CDM model (with Λ and the cold dark matter (CDM) as the dominant energy contributors [4]). Nevertheless, the type Ia supernovae data [5, 6], as well as the WMAP [7] and PLANCK results [8], do provide some room for a DE with at least a slowly time-varying equation of state (EoS) parameter w_x , on an average close to the Λ CDM value (equal to -1).

*emails: sourav@physics.du.ac.in, sourav.sur@gmail.com

†emails: asbhatia@physics.du.ac.in, arshdeepsb@gmail.com

Extensive studies of the dynamical aspects of DE have covered a wide range of models [2] commonly involving one or more scalar field(s), e.g. quintessence, k-essence, dilaton, tachyon, chameleon, etc. [9, 10, 11, 12, 13], or aerodynamic fluids, such as the Chaplygin gas and its variants [14]. Some of these have their origin traced from underlying string/M theories [15] or brane-world scenarios involving Dirac-Born-Infeld (DBI) actions [16]. Besides, there are DE models in modified/alternative theories of gravity [17] (e.g. the $f(\mathcal{R})$ theories¹ [18]), which have drawn considerable attention in recent years. In many occasions, such purely geometric theories have one-to-one mapping with scalar-tensor theories, and as such give rise to interacting dark energy-matter scenarios [19] under conformal transformations. A class of theories that comes under the alternative gravity category, is that of scalar field(s) coupled to gravity with torsion, viz. the *metric-scalar-torsion* (MST) theories [20, 21]. Our objective here is to look for cosmological models that emerge out of these theories, particularly from the DE perspective.

Torsion, which geometrically manifests the classical spin density, is a third rank (partially) antisymmetric tensor field introduced via the covariant derivative in theoretical formulations of gravity in the Riemann-Cartan space-time [22, 23]. Such theories, unlike General Relativity (GR), are characterized by an asymmetric (but metric-compatible) affine connection, a two-index antisymmetrization of which is identified as the torsion. The study of torsion has a very long history that traces back to the attempts of Cartan and Einstein, in early 1920s, to unify the fundamental interactions in the spirit of general covariance [22, 23, 24, 25]. Modern conception of torsion is often apprehended as a classical background being provided for quantized matter with spin, and as such torsion could be a low energy manifestation of a fundamental (quantum gravitational) theory [20, 26]. For instance, the massless antisymmetric Kalb-Ramond (KR) field in closed string theory is argued to be the source of a completely antisymmetric torsion in the low energy limit [27, 28]. Many implications of such a KR-induced torsion have been studied in detail, both in the four dimensional framework as well as in the extra dimensional scenarios [29, 30, 31, 32, 33, 34, 35]. Cosmology in particular being a major area of testing torsion, a few pertinent works worth special mention, viz. the torsion quintessence models [36], the $f(T)$ models in *teleparallel* theories [37], and the models based on the extended gravity theories [38] and the Poincaré gauge theory of gravity [39, 40].

We in this paper study the role of torsion, and its coupling with curvature and scalar field (i.e. the MST coupling), in explaining the dynamical evolution of DE in a self-consistent way. In particular, restricting ourselves to homogeneous and isotropic cosmologies, we examine the conditions under which the MST theory can give rise to a cosmological model with a presumably slow DE dynamics, not differing much from Λ CDM. Conversely, from a supposition that such a MST-DE model exists, we look to determine the bounds on the torsion mode parameters, and hence constrain the MST theory. Our formalism is based on the assumption of a specific non-minimal coupling of the scalar field with the four-dimensional Riemann-Cartan (or U_4) Lagrangian. This may be justified from the point of view that the (usual) minimal MST coupling encounters a uniqueness problem when it comes to defining equivalent actions upon integrating out the boundary terms in four dimensions [20]. By virtue of the non-minimal MST action, the (vector) trace mode of torsion gets sourced by the (supposedly primordial) scalar field, and hence gets eliminated via a constraint relation. Moreover, the assumption of a homogeneous and isotropic universe, described by the well-known Friedmann-Roberstson-Walker (FRW) metric, puts certain restrictions on the torsion degrees of freedom. Specifically, since the four-dimensional FRW space-time is foliated into three-dimensional maximally

¹Characterized by arbitrary functional dependence of the gravitational Lagrangian on the Ricci scalar curvature \mathcal{R} .

symmetric hypersurfaces of constant time, the torsion tensor components which uphold the maximal symmetry can only exist, and that too with a constrained coordinate dependence [41, 42, 43]. Suitable implementation of such constraints (or a few alternative ones) in the action may result in the scalar field picking up an effective mass, in addition to its inherent mass (if any), at the expense of one of the torsion modes, viz. the completely antisymmetric or the pseudo-trace mode. One is thus left with a scalar-tensor theory equivalent action that exhibits a non-minimal coupling of a massive scalar field with the Riemannian curvature scalar (\mathcal{R}) in four dimensions. We obtain specific cosmological solutions of the field equations derived from such an action, in course of building up a viable dynamic DE model. However such dynamics, is assumed be fairly weak at the cosmological scales, so that the cosmological parameters for the model are kept within the limits given by the Λ CDM error estimates from recent observations.

While dealing with the effective scalar-tensor theory, we take into account the formalisms in both the *Einstein* frame and the *Jordan* frame (in which the corresponding MST action could be reduced to the Brans-Dicke (BD) form). Whereas the Jordan frame exhibits an explicit non-minimal coupling of the scalar field with curvature, in the Einstein frame the scalar has an inherent coupling with the cosmological matter (which we consider to be the non-relativistic *dust*). Although these two frames are mathematically equivalent, being related by a conformal transformation, their physical equivalence is reinstated only by a redefinition of the units of mass, length and time under the transformation. This makes the coupling constants in one frame, evolving with time in the other. As the formulation of a physical theory in a frame with running coupling constants is generally not feasible, in the literature one often finds a rigid set of units chosen for either of the frames, which of course destroys their physical equivalence [44]. So it becomes difficult to decide which frame is suitable for interpreting observational results. Without getting into this much debated issue (which has no clear resolution till date), we use the observational results to constrain our model in both Einstein and Jordan frames, taking one or the other to be physical.

The assumption of weak DE dynamics allows us to make the parametric estimation of our model in comparison with Λ CDM. We take into account the Λ CDM parametric marginalizations due to the WMAP 9 year data [7] and the PLANCK 2015 data [8] (with combinations of high redshift supernovae of type Ia, lensing, and Baryon Acoustic Oscillations (BAO) data). We follow certain specific procedures, in which we impose, for example, the condition that the effective Hubble constant H_0 for our model to be within the 68% confidence limits of the corresponding Λ CDM Hubble constant \overline{H}_0 , for a given dataset. This in principle enables us to work out the bounds on our model parameters, and hence on the quantities of interest, such as the non-minimal coupling parameter (or equivalently, the effective BD parameter \mathfrak{w}), and the torsion parameters (that are taken to be lengths of the trace and pseudo-trace mode vectors). Although these bounds are approximate, not being derived via a full fledged likelihood analysis, they are of importance qualitatively (and to some extent quantitatively) in demonstrating the following:

- A slowly dynamical DE may result from even a small amount of torsion, via the coupling of the latter with a scalar field. As such, one may have an indirect observational signature of a fundamental theory (e.g. string theory), if torsion or(and) the scalar field is(are) considered as low energy manifestation(s) of the same.
- It suffices to consider only a mass term for the scalar field, and no other form of its potential, nor a cosmological constant, is necessary for the DE model almost identical to Λ CDM.
- The scalar field mass (or part thereof) may effectively be due to the torsion pseudo-trace mode. Hence the

latter can play a significant role in the DE evolution, as opposed to the trace mode of torsion.

Besides these, the very assumption of the weak dynamics of DE gets independent support in both Einstein and Jordan frames, as the upper limit of the non-minimal coupling parameter turns out to quite low, implying a large lower limit of the effective BD parameter \mathfrak{w} , consistent with the local gravity constraints on the latter [45, 46].

The organization of this paper is as follows: we start with the general discussion on the MST formalism in section 2, and in particular motivate the non-minimally coupled gravity-scalar field action in the Riemann-Cartan space-time. The standard cosmological setup for the MST coupling is described in section 3, in which the MST action is reduced to an equivalent scalar-tensor form by using the constraints on the torsion modes in a spatially flat FRW universe. We also make propositions for a scalar field mass term out of the torsion pseudo-trace mode, and define the effective torsion mode parameters in Jordan and Einstein frames. In section 4, we make a comprehensive study of the DE evolution in the Einstein frame. We work out first the appropriate cosmological solution for the same. Then the parametric estimations are done using a comparative analysis, taking the six parameter base Λ CDM model as the reference. We follow two procedures that depend on the choice of the cosmological parameter(s) relevant for determining the statistical bound on our model parameter. For different datasets, this bound is utilized to obtain the plots for various quantities of interest, and to study their characteristic difference with those for Λ CDM. Finally, we work out the bounds on the torsion mode parameters and the effective BD parameter (or, rather the parameter for the non-minimal coupling, from which the Einstein frame cosmology stems out). A similar analysis is done in section 5, for the Jordan frame MST cosmology. The most striking feature we notice in the Jordan frame is the effective crossing of the so-called “*phantom barrier*” which leaves us in a “*superaccelerating*” regime at the present epoch. For correlating the results of the analysis in Einstein and Jordan frames, we discuss in section 6, the difference between our approach and that of the transformation of the model parameters (and other derived quantities) under the redefinition of length, mass and time in terms of the conformal factor. We conclude with a brief summary and some open questions in section 7.

Our notations and conventions are the following: the metric signature throughout is $(-, +, +, +)$. We choose to work in units $c = 1$, whence the gravitational coupling factor is $\kappa^2 \equiv 8\pi G$, where G is the Newton’s constant. A subscript ‘0’ affixed to the cosmological quantities denotes the values of such quantities at the present epoch. The determinant of the metric tensor $g_{\mu\nu}$ is denoted by g .

2 Metric-torsion coupling with a scalar field — the general MST formalism

Let us briefly review some important aspects of the four dimensional Riemann-Cartan (U_4) space-time, which is characterized by an asymmetric affine connection $\tilde{\Gamma}_{\mu\nu}^\lambda$ ($\neq \tilde{\Gamma}_{\nu\mu}^\lambda$). A detailed formalism can be found in ref. [41].

The torsion tensor, defined by

$$T_{\mu\nu}^\lambda := 2\tilde{\Gamma}_{[\mu\nu]}^\lambda \equiv \tilde{\Gamma}_{\mu\nu}^\lambda - \tilde{\Gamma}_{\nu\mu}^\lambda, \quad (2.1)$$

can in general be decomposed as[20, 41, 47]

$$T_{\mu\nu}^\lambda = \frac{1}{3} \left(\delta_\nu^\lambda \mathcal{T}_\mu - \delta_\mu^\lambda \mathcal{T}_\nu \right) + \frac{1}{6} \epsilon^\lambda_{\mu\nu\sigma} \mathcal{A}^\sigma + \mathcal{Q}^\lambda_{\mu\nu}, \quad (2.2)$$

where $\mathcal{T}_\mu := T^\nu_{\mu\nu}$ is torsion *trace* vector mode, $\mathcal{A}^\sigma := \epsilon^{\alpha\beta\gamma\sigma} T_{\alpha\beta\gamma}$ is the torsion *pseudo-trace* vector mode, and $\mathcal{Q}_{\mu\nu\sigma}$ is the (*pseudo-tracefree*) tensorial mode of torsion.

The U_4 curvature scalar is expressed as²

$$\tilde{\mathcal{R}} := \mathcal{R} - 2\nabla_\mu \mathcal{T}^\mu - \frac{2}{3} \mathcal{T}_\mu \mathcal{T}^\mu + \frac{1}{24} \mathcal{A}_\mu \mathcal{A}^\mu + \frac{1}{2} \mathcal{Q}_{\mu\nu\sigma} \mathcal{Q}^{\mu\nu\sigma} \quad (2.3)$$

where \mathcal{R} is the four dimensional Riemannian (R_4) curvature scalar, and ∇_μ denotes the usual R_4 covariant derivative defined in terms of the Riemannian Levi Civita connection $\Gamma_{\mu\nu}^\lambda (= \Gamma_{\nu\mu}^\lambda)$. The U_4 covariant derivative $\tilde{\nabla}_\mu$, on the other hand, is defined in terms of the asymmetric connection $\tilde{\Gamma}_{\mu\nu}^\lambda$, so that the metricity condition $\tilde{\nabla}_\mu g_{\alpha\beta} = 0$ holds.

Our starting point is the action below, for the non-minimal U_4 coupling to a scalar field ϕ with a self-interacting potential $V(\phi)$:

$$\mathcal{S} = \int d^4x \sqrt{-g} \left[\frac{\beta\phi^2}{2} \tilde{\mathcal{R}} - \frac{1}{2} g^{\mu\nu} \partial_\mu \phi \partial_\nu \phi - V(\phi) \right], \quad (2.4)$$

where β is a coupling parameter. Such a non-minimal coupling may be motivated from the following:

In the four-dimensional Minkowski (M_4) space-time, with metric $\eta_{\mu\nu} = \text{diag}(-1, 1, 1, 1)$, the scalar field Lagrangian given in the standard form

$$\mathcal{L}_{(\phi)} = -\frac{1}{2} \eta^{\mu\nu} \partial_\mu \phi \partial_\nu \phi - V(\phi), \quad (2.5)$$

can equivalently be expressed, up to a divergence term, as

$$\mathcal{L}'_{(\phi)} = \frac{1}{2} \eta^{\mu\nu} \phi \partial_\mu \partial_\nu \phi - V(\phi). \quad (2.6)$$

If the scalar field is coupled to the curvature terms in the Riemannian (R_4) space-time, then under the minimal coupling (MC) scheme ($\partial_\mu \rightarrow \nabla_\mu$) the generalizations of $\mathcal{L}_{(\phi)}$ and $\mathcal{L}'_{(\phi)}$ differ by a R_4 divergence term, and their equivalence is thus maintained. However, in the Riemann-Cartan (U_4) space-time having torsion, the MC generalizations ($\partial_\mu \rightarrow \tilde{\nabla}_\mu$) of the two forms of the Lagrangian no longer remain equivalent, as their difference is not just a total divergence in U_4 , but in addition a term proportional to $\sqrt{-g} \phi^2 \nabla_\mu \mathcal{T}^\mu$ [20]. The choice of the Lagrangian for a minimally coupled metric-scalar-torsion (MST) theory therefore becomes ambiguous. The remedy to this is to modify the overall MST action by including a term that would cancel the above additional term (plus a total divergence at most). Such a modification may require one to resort to the whole exercise of suitably generalizing the standard Gibbons-Hawking-York (GHY) boundary term in presence of the torsion and scalar degrees of freedom. As an alternative however, one may simply look beyond the MC prescription, and propose a MST action explicitly having a counter-term given as a contact interaction of the scalar field with the torsion trace mode³, or at least with its covariant derivative $\nabla_\mu \mathcal{T}^\mu$. Now, it would seem quite a contrived setup if only the $\nabla_\mu \mathcal{T}^\mu$ term is picked up among the host of terms in $\tilde{\mathcal{R}}$ (given by Eq. (2.3)) and made to couple with the scalar field via a contact interaction. So to maintain regularity in the terms, we choose to couple the scalar field non-minimally to the entire U_4 Lagrangian $\sqrt{-g} \tilde{\mathcal{R}}$ in the equation (2.4) above⁴. Using now Eq. (2.2) we rewrite the MST action (2.4), up to a

²We correct a couple of misprints in Eq. (A.22) of ref. [41].

³Note that a scalar field could be minimally coupled to the U_4 action without any ambiguity when torsion is traceless, i.e. completely antisymmetric in its indices (e.g. the one that is induced by the Kalb-Ramond field in the string-inspired scenarios).

⁴More general MST actions can also be proposed [20]. However we restrain from using those as they would inevitably involve more than one coupling parameter, which may affect the predictability of the theory.

divergence term, as

$$\mathcal{S} = \int d^4x \sqrt{-g} \left[\frac{\beta\phi^2}{2} \left(\mathcal{R} + 4\mathcal{T}^\mu \frac{\partial_\mu\phi}{\phi} - \frac{2}{3}\mathcal{T}_\mu\mathcal{T}^\mu + \frac{1}{24}\mathcal{A}_\mu\mathcal{A}^\mu + \frac{1}{2}\mathcal{Q}_{\mu\nu\sigma}\mathcal{Q}^{\mu\nu\sigma} \right) - \frac{1}{2}g^{\mu\nu}\partial_\mu\phi\partial_\nu\phi - V(\phi) + \mathcal{L}^{(m)} \right], \quad (2.7)$$

where we have considered the presence of other matter fields, such as fermionic matter or cosmological fluid matter, with Lagrangian density $\mathcal{L}^{(m)}$.

3 MST theory in the standard cosmological setup

To study the cosmological consequences of the MST coupling, let us resort to the following widely accepted scenario:

1. The universe is homogeneous and isotropic at large scales, with the spatially flat FRW metric structure

$$ds^2 = -dt^2 + a^2(t) (dr^2 + r^2 d\Omega_2^2), \quad (3.1)$$

where t is the comoving time coordinate, and $a(t)$ is the cosmological scale factor.

2. The cosmological fluid matter is the pressureless *dust*, with energy density $\rho^{(m)}$ varying only with time.

As is well-known, the FRW metric describes a four-dimensional space-time foliated into three-dimensional maximally symmetric subspaces identified as hypersurfaces of constant time. For the maximal symmetry to be preserved in presence of torsion, the latter gets constrained from the requirement of its form-invariance under such symmetry. An in-depth study in ref. [41] (see also [42, 43, 48]) reveals that for determining such constraints on torsion, one may in principle resort to two schemes depending on whether torsion plays a passive or an active role in implementing the very concept of maximal symmetry. In one scheme, in which maximal symmetry is attributed solely to the metric properties of space-time, the FRW metric structure restricts torsion to have at most four non-vanishing independent components, viz. $T_{110}, T_{220}, T_{330}$ and T_{123} , each of which can depend on time only. In the other scheme, in which torsion directly affects maximal symmetry, following strictly the principle of general covariance, some more independent torsion components with only time-dependence, viz. T_{001}, T_{002} and T_{003} , are allowed in the FRW context [41]. Hence, for the irreducible torsion modes, one finds that both the schemes are in agreement yielding $\mathcal{Q}_{\mu\nu\sigma} = 0$ and $\mathcal{A}^\mu = \delta_0^\mu \lambda(t)$ where $\lambda(t)$ is a pseudoscalar function of time. The disagreement comes when one scheme allows only the \mathcal{T}_0 component of the torsion trace vector \mathcal{T}_μ , whereas the other scheme allows all the components (with some restrictions though). However, this is not a concern for us since we are considering the cosmological matter to be the non-relativistic dust, having no explicit dependence on torsion. As such, \mathcal{T}_μ being an auxiliary field in the MST action (2.7), satisfies the constraint equation

$$\mathcal{T}_\mu = 3 \frac{\partial_\mu\phi}{\phi}, \quad (3.2)$$

which when substituted, alongwith the constraint $\mathcal{Q}_{\mu\nu\sigma} = 0$, back in Eq. (2.7) gives the on-shell action

$$\mathcal{S} = \int d^4x \sqrt{-g} \left[\frac{\beta\phi^2}{2} \left(\mathcal{R} + \frac{1}{24}\mathcal{A}_\mu\mathcal{A}^\mu \right) - \frac{(1-6\beta)}{2} g^{\mu\nu}\partial_\mu\phi\partial_\nu\phi - V(\phi) + \mathcal{L}^{(m)} \right]. \quad (3.3)$$

This has an arbitrariness left in it though, viz. the choice of the scalar potential $V(\phi)$. Now, in analogy with the gravitational field, torsion is conventionally taken to be massless [22, 26]. In the MST context therefore, since the scalar field ϕ acts as the source of the trace mode of torsion (by virtue of the relation (3.2)), one expects ϕ to be massless as well. We however make the allowance for ϕ to have a mass m_ϕ , i.e.

$$V(\phi) = \frac{1}{2} m_\phi^2 \phi^2 . \quad (3.4)$$

In fact, a scalar field mass term may be induced effectively in the FRW space-time, at the expense of the torsion pseudo-trace mode \mathcal{A}^μ , as demonstrated below.

3.1 Effective scalar field mass via torsion pseudo-trace

The above constraint $\mathcal{A}^\mu = \delta_0^\mu \lambda(t)$ can in principle be implemented in the theory by using a Lagrange multiplier field \mathfrak{L}_μ . Now, in the literature one often finds that phenomenological studies are done with the approximation of a constant (or very weakly evolving) torsion background [20, 30, 31, 49, 50]. In the same spirit we may therefore make an additional assumption that the pseudoscalar $\lambda(t)$ is rolling so slowly that it may effectively be replaced with its average $\langle \lambda \rangle$ over a very large cosmological time-scale (possibly stretching well past the redshift of last scattering $z_{LS} \simeq 1089$, so that dust cosmologies would not get affected anyway). In other words, we invoke a modified constraint $\mathcal{A}^\mu = \delta_0^\mu \langle \lambda \rangle$ in the action (3.3), by augmenting the latter with a Lagrange multiplier term, The \mathcal{A}^μ -dependent part of (3.3), with the augmentation, is then

$$\mathcal{S}_\mathcal{A} = \int d^4x \sqrt{-g} \left[\frac{\beta \phi^2}{48} \mathcal{A}_\mu \mathcal{A}^\mu + \mathfrak{L}_\mu (\mathcal{A}^\mu - \delta_0^\mu \langle \lambda \rangle) \right] . \quad (3.5)$$

From this, it follows that in the FRW space-time we have

$$\mathfrak{L}_\mu = -\frac{\beta \phi^2}{24} \mathcal{A}_\mu = \left(\frac{\langle \lambda \rangle \beta \phi^2}{24}, 0, 0, 0 \right) , \quad (3.6)$$

and the above part (3.5) of the MST action written on-shell as

$$\mathcal{S}_\mathcal{A} = - \int dt \int d^3x a^3(t) \left[\frac{1}{2} m_\mathcal{A}^2 \phi^2(t) \right] . \quad (3.7)$$

This resembles the action for the potential part of the scalar field ϕ representing effectively a mass, which is given by the constant

$$m_\mathcal{A} = \langle \lambda \rangle \sqrt{\frac{\beta}{24}} . \quad (3.8)$$

Such a mass-like term however has conformal properties different from that of the usual scalar field mass term (3.4). One may in fact note that Eq. (3.7) holds only for the FRW space-time metric in comoving coordinates (with constant lapse function). In other space-times (or coordinate systems), the on-shell Lagrangian would carry a factor proportional to the metric component g_{00} , and would therefore get affected in a different way than a scalar field mass term under conformal transformations⁵. As possible alternative ways of inducing, via the \mathcal{A}^μ mode, a mass term for the scalar field ϕ with its usual conformal properties preserved, we may resort to one of the following:

⁵This is reminiscent of the rather simple metric-torsion cosmological setup in [20, 51], involving only the completely antisymmetric torsion mode (i.e. the pseudo-trace \mathcal{A}^μ). For a contact interaction of \mathcal{A}^μ with a conformally constant spinor current J^μ , assumed therein, the ensuing constraint equation implies that J^μ has its norm acting as a cosmological constant, albeit with different conformal properties.

Proposition 1: Refer for instance to some variants of the vector-tensor gravity theories, viz. the Einstein-æther theories [52, 53, 54], in which a *fixed* expectation value for a time-like vector field (dubbed “æther”) is enforced via a norm-fixing constraint, using a Lagrange multiplier. For the torsion pseudo-trace vector \mathcal{A}^μ , we can implement a similar norm-fixing constraint

$$\mathcal{A}_\mu \mathcal{A}^\mu = -\langle \lambda \rangle^2, \quad (3.9)$$

which, by the analogy of æther, would fix the field mode \mathcal{A}^μ at an expectation value $\langle \lambda \rangle$, supposedly in an underlying quantum theory of gravity (with torsion). Incorporating such a constraint in the action (3.3), by the use of a Lagrange multiplier \mathfrak{L} , one gets the on-shell action similar to Eq. (3.7):

$$\mathcal{S}_\mathcal{A} = - \int d^4x \sqrt{-g} \left[\frac{1}{2} m_\mathcal{A}^2 \phi^2(t) \right], \quad (3.10)$$

with the mass $m_\mathcal{A}$ given by Eq. (3.8), but without any allusion to the FRW (or any other specific) metric structure. So we have an effective contribution to the mass of the scalar field ϕ , but now with the mass term having its “generic” interpretation, as it preserves the properties of a usual scalar mass term under a conformal transformation.

Proposition 2: Consider, for example, incorporating quadratic order torsion term(s) in the MST action (3.3). For simplicity, let us take into account only the square of $\mathcal{A}_\mu \mathcal{A}^\mu$, so that the \mathcal{A}^μ -dependent part of (3.3) becomes

$$\mathcal{S}_\mathcal{A} = \int d^4x \sqrt{-g} \left(\frac{\beta \phi^2}{2} \right) \left[\frac{1}{24} \mathcal{A}_\mu \mathcal{A}^\mu + \gamma \mathcal{A}_\mu \mathcal{A}^\mu \mathcal{A}_\nu \mathcal{A}^\nu \right], \quad (3.11)$$

where γ is a coupling constant having the dimension of ϕ^2 . One obtains the non-trivial constraint

$$\mathcal{A}_\mu \mathcal{A}^\mu = -\frac{1}{48\gamma}, \quad (3.12)$$

and consequently the on-shell action is the same as Eq. (3.10), but with the scalar field mass

$$m_\mathcal{A} = \frac{1}{48} \sqrt{\frac{\beta}{\gamma}}. \quad (3.13)$$

In accordance with these propositions, we can in principle have an effective potential for the scalar field given by

$$V_{\text{eff}}(\phi) = V(\phi) + \frac{\beta \phi^2}{48} \mathcal{A}_\mu \mathcal{A}^\mu + \text{suitable augmentations} = \frac{1}{2} m^2 \phi^2, \quad (3.14)$$

with the effective mass $m = \sqrt{m_\phi^2 + m_\mathcal{A}^2}$, in general.

It should however be pointed out here that there could be more alternative ways to assign a mass term for the scalar field. The above propositions depict only some exemplary scenarios, and do not put a stringent claim that the torsion pseudo-trace \mathcal{A}^μ would always induce the scalar field mass. We shall neither attempt to explain the origin of m_ϕ , nor try to assert the source of \mathcal{A}^μ (or the origin of $m_\mathcal{A}$) any further in this work.

3.2 Effective scalar-tensor theoretical framework

Under the mass term consideration for the scalar field ϕ , and the elimination of the mode \mathcal{A}^μ via a constraint (as discussed above), we are left with the on-shell action

$$\mathcal{S} = \int d^4x \sqrt{-g} \left[\frac{\beta\phi^2}{2} \mathcal{R} - \frac{(1-6\beta)}{2} g^{\mu\nu} \partial_\mu \phi \partial_\nu \phi - \frac{1}{2} m^2 \phi^2 + \mathcal{L}^{(m)} \right]. \quad (3.15)$$

This is of course the action of a scalar-tensor theory in the original *Jordan* frame [44], which is characterized by a running gravitational coupling parameter

$$G_{\text{eff}}(t) = G \left[\frac{\phi_0}{\phi(t)} \right]^2, \quad (3.16)$$

defined so that at the present epoch $t = t_0$, we have $G_{\text{eff}}(t_0) = G$, the Newton's constant, under the stipulation

$$\phi(t_0) \equiv \phi_0 = \frac{1}{\kappa\sqrt{\beta}}, \quad \text{with} \quad \kappa = \sqrt{8\pi G}. \quad (3.17)$$

If one redefines the scalar field as

$$\Phi(t) := \Phi_0 \left[\frac{\phi(t)}{\phi_0} \right]^2, \quad \text{with} \quad \Phi_0 \equiv \Phi(t_0) = \beta\phi_0^2 = \kappa^{-2}, \quad (3.18)$$

then Eq. (3.15) reduces to an equivalent *Brans-Dicke* (BD) action (albeit with a potential for Φ) [44]:

$$\mathcal{S} = \int d^4x \sqrt{-g} \left[\frac{\Phi \mathcal{R}}{2} - \frac{\mathfrak{w}}{2\Phi} g^{\mu\nu} \partial_\mu \Phi \partial_\nu \Phi - \mathcal{V}(\Phi) + \mathcal{L}^{(m)} \right], \quad (3.19)$$

where \mathfrak{w} is the effective BD parameter, given by

$$\mathfrak{w} = \frac{1}{4\beta} - \frac{3}{2}, \quad (3.20)$$

and the scalar field potential is

$$\mathcal{V}(\Phi) = \mathcal{V}_0 \frac{\Phi}{\Phi_0}, \quad \text{with} \quad \mathcal{V}_0 \equiv \mathcal{V}(\Phi)|_{t=t_0} = \frac{1}{2} m^2 \phi_0^2. \quad (3.21)$$

The corresponding equations of motion are

$$\mathcal{R}_{\mu\nu} = \frac{1}{\Phi} \left[T_{\mu\nu}^{(m)} - (\mathfrak{w} + 1) g_{\mu\nu} \square\Phi + \nabla_\mu \partial_\nu \Phi + \frac{\mathfrak{w}}{\Phi} \partial_\mu \Phi \partial_\nu \Phi \right], \quad (3.22)$$

$$\square\Phi = \frac{1}{2\mathfrak{w} + 3} \left[T^{(m)} - 2\mathcal{V}(\Phi) \right], \quad (3.23)$$

where

$$T_{\mu\nu}^{(m)} = -\frac{2}{\sqrt{-g}} \frac{\delta}{\delta g^{\mu\nu}} \left[\sqrt{-g} \mathcal{L}^{(m)} \right], \quad (3.24)$$

with trace $T^{(m)} = g^{\mu\nu} T_{\mu\nu}^{(m)}$, is the matter stress-energy tensor, which is conserved:

$$\nabla_\alpha \left(g^{\alpha\nu} T_{\mu\nu}^{(m)} \right) = 0. \quad (3.25)$$

As the cosmological fluid is considered here to be the pressureless dust, we have

$$T_{\mu\nu}^{(m)} = \rho^{(m)} u_\mu u_\nu, \quad \text{and} \quad T^{(m)} = -\rho^{(m)}, \quad (3.26)$$

where $\rho^{(m)}$ is the dust energy density, and u^μ is the four velocity vector which satisfies $g_{\mu\nu}u^\mu u^\nu = -1$.

Refer back again to Eq. (3.15), which under a conformal transformation

$$g_{\mu\nu} \longrightarrow \widehat{g}_{\mu\nu} = \left(\frac{\phi}{\phi_0}\right)^2 g_{\mu\nu}, \quad (3.27)$$

reduces to the scalar-tensor action in the so-called *Einstein* frame:

$$\widehat{S} = \int d^4x \sqrt{-\widehat{g}} \left[\frac{\widehat{\mathcal{R}}}{2\kappa^2} - \frac{1}{2} \left(\frac{\phi_0}{\phi}\right)^2 \widehat{g}^{\mu\nu} \partial_\mu \phi \partial_\nu \phi - \frac{m^2 \phi_0^2}{2} \left(\frac{\phi_0}{\phi}\right)^2 + \left(\frac{\phi_0}{\phi}\right)^4 \mathcal{L}^{(m)}(\widehat{g}, \phi) \right], \quad (3.28)$$

where $\widehat{g} \equiv \det(\widehat{g}_{\mu\nu})$, and $\widehat{\mathcal{R}} = \widehat{g}^{\mu\nu} \widehat{\mathcal{R}}_{\mu\nu}$ with $\widehat{\mathcal{R}}_{\mu\nu}$ the Ricci tensor constructed using $\widehat{g}_{\mu\nu}$. Note that $\mathcal{L}^{(m)}$ is now in general a function of both $\widehat{g}_{\mu\nu}$ and ϕ . Redefining, without loss of generality, the scalar field as

$$\varphi := \phi_0 \ln \left(\frac{\phi}{\phi_0}\right), \quad \text{such that} \quad \varphi(t_0) = 0, \quad (3.29)$$

the Einstein frame action (3.28) can be expressed in a more convenient form:

$$\widehat{S} = \int d^4x \sqrt{-\widehat{g}} \left[\frac{\widehat{\mathcal{R}}}{2\kappa^2} - \frac{1}{2} \widehat{g}^{\mu\nu} \partial_\mu \varphi \partial_\nu \varphi - \mathcal{U}(\varphi) + \widehat{\mathcal{L}}^{(m)}(\widehat{g}, \varphi) \right], \quad (3.30)$$

with the corresponding matter Lagrangian density

$$\widehat{\mathcal{L}}^{(m)}(\widehat{g}, \varphi) = e^{-4\varphi/\phi_0} \mathcal{L}^{(m)}(\widehat{g}, \phi(\varphi)) = e^{-2\kappa\sqrt{\beta}\varphi} \mathcal{L}^{(m)}(\widehat{g}, \phi(\varphi)), \quad (3.31)$$

and the scalar field potential given as

$$\mathcal{U}(\varphi) = \mathcal{U}_0 e^{-2\varphi/\phi_0} = \mathcal{U}_0 e^{-2\kappa\sqrt{\beta}\varphi}, \quad \text{where} \quad \mathcal{U}_0 \equiv \mathcal{U}(\varphi)|_{t=t_0} = \frac{m^2 \phi_0^2}{2} = \frac{m^2}{2\kappa^2 \beta}. \quad (3.32)$$

One derives the following equations of motion in the Einstein frame:

$$\widehat{\mathcal{R}}_{\mu\nu} = \kappa^2 \left[\widehat{T}_{\mu\nu}^{(m)} - \frac{1}{2} \widehat{g}_{\mu\nu} \widehat{T}^{(m)} + \partial_\mu \varphi \partial_\nu \varphi + g_{\mu\nu} \mathcal{U}(\varphi) \right], \quad (3.33)$$

$$\widehat{\nabla}_\alpha \left(\widehat{g}^{\alpha\nu} \widehat{T}_{\mu\nu}^{(m)} \right) = -\kappa \sqrt{\beta} \widehat{T}^{(m)} \partial_\mu \varphi. \quad (3.34)$$

The corresponding matter stress-energy tensor, viz.

$$\widehat{T}_{\mu\nu}^{(m)} = -\frac{2}{\sqrt{-\widehat{g}}} \frac{\delta}{\delta \widehat{g}^{\mu\nu}} \left[\sqrt{-\widehat{g}} \widehat{\mathcal{L}}^{(m)} \right], \quad (3.35)$$

with trace $\widehat{T}^{(m)} = \widehat{g}^{\mu\nu} \widehat{T}_{\mu\nu}^{(m)}$, is not conserved though, as is evident from Eq. (3.34). For the non-relativistic dust

$$\widehat{T}_{\mu\nu}^{(m)} = \widehat{\rho}^{(m)} \widehat{u}_\mu \widehat{u}_\nu, \quad \text{and} \quad \widehat{T}^{(m)} = -\widehat{\rho}^{(m)}, \quad (3.36)$$

where $\widehat{\rho}^{(m)}$ and \widehat{u}^μ are respectively the Einstein frame dust energy density and four velocity, the latter satisfying $\widehat{g}_{\mu\nu} \widehat{u}^\mu \widehat{u}^\nu = -1$. One may verify that $\widehat{T}_{\mu\nu}^{(m)}$, $\widehat{\rho}^{(m)}$ and \widehat{u}^μ hold the following relationships with the corresponding quantities in the Jordan frame [44]:

$$T_{\mu\nu}^{(m)} = e^{2\kappa\sqrt{\beta}\varphi} \widehat{T}_{\mu\nu}^{(m)}, \quad \rho^{(m)} = e^{4\kappa\sqrt{\beta}\varphi} \widehat{\rho}^{(m)}, \quad \text{and} \quad u^\mu = e^{\kappa\sqrt{\beta}\varphi} \widehat{u}^\mu. \quad (3.37)$$

The Einstein frame is of course more convenient to work on, than the Jordan frame which has rather unusual features, due to the running gravitational coupling parameter. The Einstein's equations that can be handled in a familiar way in the Einstein frame, are subject to some abstruseness due to the non-minimal gravitational coupling with a scalar field in the Jordan frame. This consequently makes a characteristic difference between the cosmologies in the two frames. However, amidst its bizarreness, the Jordan frame cosmology shows one regularity, viz. the conserved stress-energy tensor of the fluid matter. In the Einstein frame, the scalar field is made to couple with gravity in the usual minimal way, but at the expense of its interaction with the fluid. Moreover, the original non-minimal scalar-gravity coupling parameter β is still traced in the Einstein frame, as it appears in the expression (3.32) for the scalar potential as well as in the matter conservation relation (3.34).

In what follows, we shall analyse in section 4 the Einstein frame cosmological solutions of the field equations in the MST context, with emphasis on a viable dark energy model build-up. Subsequently, in section 5 an analogous study in the Jordan frame would be performed, not just for completeness but also to restrain ourselves from making a preference whilst a longstanding debate on the physical relevance of the two frames prevails. Our focus would be on the estimation of the cosmological model parameters, and hence on obtaining specific bounds on the effective Brans-Dicke parameter and the torsion mode parameters (given by the norms of the vectors \mathcal{T}_μ and \mathcal{A}^μ). The precise expressions for the latter, in both the frames, are worked out in the following subsection.

3.3 Effective torsion mode parameters

The effective scalar-tensor formulation of the MST theory somewhat obscures the torsion vector modes \mathcal{T}_μ and \mathcal{A}^μ , which are the key MST constituents. A quantitative study of these modes and their cosmological consequences requires their appropriate parametrization in the MST cosmological setup. One may look to define the density parameters for \mathcal{T}_μ and \mathcal{A}^μ and analyze them accordingly. However, that may not be a suitable approach, as these modes are interacting with the scalar field and even with the cosmological fluid (in the Einstein frame). Much serenity would be there if we just resort to finding the norms of the vectors \mathcal{T}_μ and \mathcal{A}^μ . In general a difficulty is still there though, the lengths of vector fields not being defined uniquely in conformally transformed frames. For the torsion modes however, we may choose to take the norms of \mathcal{T}_μ and \mathcal{A}^μ as defined in the Jordan frame. We then simply have in the Einstein frame, the expressions for these norms recast in terms of the corresponding metric tensor components. This is justified, since our starting point had been an explicit non-minimal coupling of the scalar field ϕ with curvature and torsion, which is perceptible in the equivalent scalar-tensor formulation of the MST theory only in the Jordan frame. Moreover, in such a formulation the mode T_μ has its norm contributing to the kinetic part of the scalar field Lagrangian density, by virtue of the constraint relation (3.2). On the other hand, the norm of A^μ contributes to the scalar field potential (or more specifically, the mass).

- **Norm of the trace vector:** Using the constraint (3.2), we have the norm of \mathcal{T}_μ expressed in the Jordan frame as

$$|\mathcal{T}| := \sqrt{-g^{\mu\nu} \mathcal{T}_\mu \mathcal{T}_\nu} = \frac{3}{\phi} \sqrt{-g^{\mu\nu} \partial_\mu \phi \partial_\nu \phi}, \quad (3.38)$$

or more conveniently, in terms of the Brans-Dicke scalar field Φ [cf. Eq. (3.18)], as

$$|\mathcal{T}| = \frac{3}{2\Phi} \sqrt{-g^{\mu\nu} \partial_\mu \Phi \partial_\nu \Phi}. \quad (3.39)$$

In the Einstein frame, we have the norm of \mathcal{T}_μ expressed in accord with Eq. (3.27):

$$|\mathcal{T}| := \left(\frac{\phi}{\phi_0} \right) \sqrt{-\hat{g}^{\mu\nu} \mathcal{T}_\mu \mathcal{T}_\nu} = \frac{3}{\phi_0} \sqrt{-\hat{g}^{\mu\nu} \partial_\mu \phi \partial_\nu \phi}. \quad (3.40)$$

Recalling now that $\phi_0 = (\kappa\sqrt{\beta})^{-1}$ [cf. Eq. (3.17)], and using the relation (3.29), $|\mathcal{T}|$ is given in terms of the Einstein frame scalar field φ as

$$|\mathcal{T}| = 3\kappa\sqrt{\beta} e^{\kappa\sqrt{\beta}\varphi} \sqrt{-\hat{g}^{\mu\nu} \partial_\mu \varphi \partial_\nu \varphi}. \quad (3.41)$$

- **Norm of the pseudo-trace vector:** Both the propositions above imply that the norm of A^μ is constant (albeit with different numerical factors) in the FRW space-time. Using Eqs. (3.8), (3.9), (3.12) and (3.13), we have (in both Jordan and Einstein frames),

$$|\mathcal{A}| := \sqrt{-g^{\mu\nu} \mathcal{A}_\mu \mathcal{A}_\nu} = \left(\frac{\phi}{\phi_0} \right) \sqrt{-\hat{g}^{\mu\nu} \mathcal{A}_\mu \mathcal{A}_\nu} = \begin{cases} \sqrt{24} \kappa m_{\mathcal{A}} \phi_0, & \text{(proposition 1)}, \\ \sqrt{48} \kappa m_{\mathcal{A}} \phi_0, & \text{(proposition 2)}. \end{cases} \quad (3.42)$$

If we assume that the scalar field mass to be solely due to the mode \mathcal{A}^μ , i.e. $m = m_{\mathcal{A}}$, then recalling that $m^2 \phi_0^2 = 2\mathcal{V}_0 \equiv 2\mathcal{U}_0$ (by Eqs. (3.21) and (3.32)), we have

$$|\mathcal{A}| = 4\kappa\sqrt{3q\mathcal{V}_0} \equiv 4\kappa\sqrt{3q\mathcal{U}_0}, \quad (3.43)$$

with $q = 1, 2$ (corresponding to propositions 1 and 2 respectively).

It is worth mentioning here that for the DE interpretation of the scalar degree of freedom within the FRW framework, the mass of the scalar field plays the key role compared to the kinetic part. Therefore, $|\mathcal{A}|$ would be much more dominant than $|\mathcal{T}|$, if we assume that the scalar field mass as the effect of \mathcal{A}^μ only. Else, the inherent scalar field mass m_ϕ would prevail over both $|\mathcal{T}|$ and $|\mathcal{A}|$, if they are supposed to be of the same order of magnitude.

4 MST Cosmology in the Einstein frame

The general setup discussed above enables us to look for exact solution(s) of the cosmological equations in presence of the MST coupling. In this section, we choose to work in the Einstein frame, supposing it to be suitable for interpreting the results of physical observations. Our objective is to seek whether the MST coupling can lead to a DE model consistent with the observational results, or conversely to determine the specific bounds on the torsion mode parameters from the supposition that a self-consistent DE model emerges out in the MST cosmological scenario. Of course, given the miniscule experimental support for torsion in many other searches, one expects the MST-DE model to be a slight modification of the concordance Λ CDM model. We therefore take the observed best-fit values of the Λ CDM cosmological parameters as the basic measures for parametric estimations of the MST-DE model, which however has one unusual feature in the Einstein frame, viz. the interaction of the DE and the cosmological matter. So we need to define the effective uncoupled DE and matter densities for the comparative study of the corresponding quantities in the Λ CDM case. This is a mathematical exercise though, and for notational simplicity we also drop the hats over all the Einstein frame quantities and operators throughout this section.

4.1 Cosmological equations and solution

The Friedmann and Raychaudhuri equations follow straightaway from Eqs. (3.33), on using the relations (3.36):

$$H^2(t) = \frac{\kappa^2}{3} \left[\rho^{(m)}(t) + \frac{\dot{\varphi}^2(t)}{2} + \mathcal{U}(\varphi(t)) \right], \quad (4.1)$$

$$\dot{H}(t) = -\frac{\kappa^2}{2} \left[\rho^{(m)}(t) + \dot{\varphi}^2(t) \right], \quad (4.2)$$

where $H(t) := \dot{a}(t)/a(t)$ is the Hubble parameter (the overhead dot $\{\cdot\}$ denotes d/dt everywhere).

The conservation equation (3.34) integrates to give

$$\rho^{(m)}(a) = \frac{\rho_0^{(m)}}{a^3} e^{-\kappa\sqrt{\beta}\varphi(a)}, \quad (4.3)$$

where $\rho_0^{(m)} = \rho^{(m)}|_{t=t_0} = \rho^{(m)}|_{a=1}$ is the present-day value of the matter density.

Assuming now a simple power-law ansatz:

$$e^{\kappa\sqrt{\beta}\varphi(a)} = a^s, \quad \text{with} \quad s = \text{a constant}, \quad (4.4)$$

a few rearrangement of terms in Eqs. (4.1) and (4.2), and algebraic steps, would lead to

$$H^2(a) = \frac{\kappa^2}{3} \left(1 - \frac{s^2}{6\beta} \right)^{-1} \left[\frac{\rho_0^{(m)}}{a^{3+s}} + \frac{\mathcal{U}_0}{a^{2s}} \right], \quad (4.5)$$

$$[a^6 H^2(a)]' = \kappa^2 \left[\rho_0^{(m)} a^{2-s} + 2\mathcal{U}_0 a^{5-2s} \right], \quad (4.6)$$

where the prime $\{'\}$ denotes d/da , and we have recalled the expression (3.32) for the scalar field potential $\mathcal{U}(\varphi)$.

It is easy to verify that a non-trivial solution can be obtained only for

$$s = 2\beta, \quad (4.7)$$

whence the Friedmann equation (4.1) [or (4.5)] becomes

$$H^2(a) = \frac{\kappa^2}{3-s} \left[\frac{\rho_0^{(m)}}{a^{3+s}} + \frac{\mathcal{U}_0}{a^{2s}} \right]. \quad (4.8)$$

This is however of a rather unusual form, because of the interaction of the scalar field with the dust. Also, the validity of Eq. (4.8) requires $s < 3$, i.e. $\beta < 3/2$, which puts a (somewhat less stringent) theoretical restriction $\mathfrak{w} > -4/3$, on the effective Brans-Dicke parameter \mathfrak{w} [given by Eq. (3.20)]. Rigorous bounds on \mathfrak{w} can in principle be obtained while matching the theoretical predictions with the observational results, as we shall see shortly. A comparison of such bounds with the local gravity constraints on \mathfrak{w} would be an independent consistency check of the MST-cosmological DE model we are studying here.

As our analysis in this section is based on the supposition that the Einstein frame is the one suited for explaining the observational results, we conveniently define an effective matter density (in the usual form) as

$$\rho_{\text{eff}}^{(m)}(a) := \rho_0^{(m)} a^{-3}, \quad (4.9)$$

and a surplus density (considered here to be the effective DE density) as

$$\rho_X(a) := \left(1 - \frac{s}{3}\right)^{-1} \left[\frac{\mathcal{U}_0}{a^{2s}} + \frac{\rho_0^{(m)}}{a^3} \left(a^{-s} - 1 + \frac{s}{3}\right) \right], \quad (4.10)$$

so that the critical density of the universe is given by

$$\rho_C(a) := \frac{3H^2(a)}{\kappa^2} = \rho_{\text{eff}}^{(m)}(a) + \rho_X(a). \quad (4.11)$$

Defining further an effective DE pressure p_X as

$$p_X(a) := - \left(1 - \frac{s}{3}\right)^{-1} \left[\left(1 - \frac{2s}{3}\right) \frac{\mathcal{U}_0}{a^{2s}} - \frac{s}{3} \frac{\rho_0^{(m)}}{a^{3+s}} \right], \quad (4.12)$$

we express the conservation equation for the above critical density in the standard form (assuming that significant contributions to the energy budget of the universe are provided only by the DE and the pressureless fluid):

$$\rho'_C(a) + \frac{3}{a} [\rho_C(a) + p_X(a)] = 0. \quad (4.13)$$

4.2 Effective cosmological parameters

The equations (4.8) – (4.12) lead us to the effective DE equation of state (EoS) parameter w_X , as a function of the redshift $z = (a^{-1} - 1)$:

$$w_X(z) := \frac{p_X(z)}{\rho_X(z)} = -1 + \frac{2s}{3} + \frac{\Omega_{\text{eff}}^{(m)}(z)}{1 - \Omega_{\text{eff}}^{(m)}(z)} \left[(1+z)^s - 1 + \frac{2s}{3} \right]. \quad (4.14)$$

with the effective matter density parameter $\Omega_{\text{eff}}^{(m)}(z)$ defined as

$$\Omega_{\text{eff}}^{(m)}(z) := \frac{\rho_{\text{eff}}^{(m)}(z)}{\rho_C(z)} = \Omega_0^{(m)} \frac{(1+z)^3}{\mathfrak{H}^2(z)}, \quad (4.15)$$

where $\Omega_0^{(m)}$ is the value of $\Omega_{\text{eff}}^{(m)}$ at the present epoch $t = t_0$ (i.e. $a = 1$, or $z = 0$), and

$$\mathfrak{H}(z) \equiv \frac{H(z)}{H_0} = \left(1 - \frac{s}{3}\right)^{-1/2} \left[\Omega_0^{(m)} (1+z)^{3+s} + \left(1 - \frac{s}{3} - \Omega_0^{(m)}\right) (1+z)^{2s} \right]^{1/2}, \quad (4.16)$$

is the rationalized Hubble parameter, $H_0 \equiv H(z=0)$ being the Hubble constant.

Substituting Eq. (4.16) back in Eq. (4.15) and simplifying, we have the following expression for the effective matter density parameter

$$\Omega_{\text{eff}}^{(m)}(z) = \frac{\Omega_0^{(m)} (1+z)^{3-2s}}{1 + \Omega_0^{(m)} \left(1 - \frac{s}{3}\right)^{-1} \left[(1+z)^{3-s} - 1 \right]}, \quad (4.17)$$

and the actual (interacting) matter density parameter is related to this as

$$\Omega^{(m)}(z) := \frac{\rho^{(m)}(z)}{\rho_C(z)} = (1+z)^s \Omega_{\text{eff}}^{(m)}(z), \quad (4.18)$$

so that at the present epoch ($z = 0$) we have $\Omega_{\text{eff}}^{(m)}(0) = \Omega^{(m)}(0) = \Omega_0^{(m)}$.

The EoS parameter for the system, worked out as

$$\mathbf{w}(z) := \frac{p_X(z)}{\rho_C(z)} = \left[1 - \Omega_{\text{eff}}^{(m)}(z)\right] \mathbf{w}_X(z) = -1 + \frac{2s}{3} + \Omega^{(m)}(z), \quad (4.19)$$

makes implicit the following:

From the requirement $\mathbf{w}(0) < -1/3$, so that the expansion of the universe is accelerating at the present epoch ($z = 0$), one gets

$$s + \frac{3}{2}\Omega_0^{(m)} < 1. \quad (4.20)$$

This means that $0 < s < 1$, because $\Omega_0^{(m)}$ is positive definite and the parameter s is presumably such⁶. So we have a constraint on s tighter than the previous one ($s < 3$). As such, the bound on the BD parameter gets tighter, viz. $\mathbf{w} > -1$, than that obtained previously ($\mathbf{w} > -4/3$). Tighter still it could be, considering that most observational probes (if not all) predict the universe being dominated by both dark energy and (baryonic plus cold dark) matter at present. That is, $\Omega_0^{(m)} \sim 1$, meaning s cannot have a large fractional value (close to 1). If, let us say, we take $\Omega_0^{(m)} \simeq 0.3$ as the fiducial value of the matter density parameter at the present epoch, then Eq. (4.20) gives $s \lesssim 1/2$, whence $\mathbf{w} \gtrsim -1/2$. Moreover, by Eq. (4.14) the present-day value of the DE EoS parameter is constrained for $\Omega_0^{(m)} \simeq 0.3$ as

$$\mathbf{w}_X(0) = -1 + \frac{2s}{3(1 - \Omega_0^{(m)})} \lesssim -\frac{1}{2}. \quad (4.21)$$

This is of course nothing new — the same bound applies to all barotropic DE models simply by virtue of the relation $\mathbf{w}(z) = \left[1 - \Omega_{\text{eff}}^{(m)}(z)\right] \mathbf{w}_X(z)$ and by the requirement $\mathbf{w}(0) < -1/3$. Therefore, like in any other DE model, we have here a fairly large scope of deviation from the Λ CDM model (in which the DE EoS parameter is fixed at -1). We however restrict ourselves to the MST induced small parametric fluctuations over Λ CDM, relying on the general consensus that the latter presently stands out as the observationally favoured model of DE. In other words, we presume the parameter s to be quite small, which is also corroborated by a very large lower bound on the BD parameter ($\mathbf{w} \gtrsim 40$ to even $\mathbf{w} \gtrsim 40000$) obtained independently⁷ from the solar system tests and other probes [45, 46].

4.3 Parametric estimation using the Λ CDM observational limits

As mentioned earlier, we in this paper are interested primarily on a order of magnitude estimate of s (and hence of the bounds on the torsion parameters). Therefore, instead of a full fledged likelihood analysis with the observational data, it would suffice us to compare the parameters of our model with those of a reference model. We choose the reference to be the six parameter Λ CDM model, which is generally taken as the base theoretical model for the observational probes. Assuming then that the cosmological parameters of our DE model are within the 68% confidence limits of the corresponding ones in the Λ CDM model for various datasets (or their combinations), we

⁶As $s = 2\beta$, a negative value of s would imply $\beta < 0$, i.e. we have the *wrong* sign for the gravity action that is coupled non-minimally to the scalar field. The underlying quantum theory would then be unbounded from below, and therefore discarded.

⁷Mostly for the massless Brans-Dicke however.

can in principle obtain the respective upper bound on the parameter s . Of course, the legitimacy of such a bound would imply the smallness of its numerical value, as one may note that the Λ CDM equations are recovered in the limit $s \rightarrow 0$ of our model. Refer for instance to the Friedmann equation (4.8), whose limiting version (expressed in terms of the redshift z):

$$\overline{H}^2(z) \equiv \lim_{s \rightarrow 0} H^2(z) = \frac{\kappa^2}{3} \left[\rho_0^{(m)} (1+z)^3 + \mathcal{U}_0 \right], \quad (4.22)$$

is nothing but the Friedmann equation of the Λ CDM model, with the cosmological constant Λ identified as \mathcal{U}_0 . Here \overline{H} denotes the Λ CDM Hubble parameter, and from now on we shall denote every Λ CDM cosmological parameter by an overbar $\{\overline{\quad}\}$, for e.g. the Λ CDM matter density parameter as $\overline{\Omega}^{(m)}$, the Λ CDM EoS parameter as \overline{w} , the Λ CDM Hubble constant as \overline{H}_0 , and so on. The relationship between \overline{H}_0 and the Hubble constant $H_0 = H(z=0)$ of our model can be traced out from Eqs. (4.8) and (4.22):

$$\overline{H}_0 = H_0 \sqrt{1 - \frac{s}{3}}. \quad (4.23)$$

Similarly, Eq. (4.17) can be expressed as a relation between $\Omega_{\text{eff}}^{(m)}(z)$ and $\overline{\Omega}^{(m)}(z)$:

$$\Omega_{\text{eff}}^{(m)}(z) = \frac{(3-s)(1+z)^{3-2s} \overline{\Omega}^{(m)}(z)}{\left[3(1+z)^{3-s} - s \right] \overline{\Omega}^{(m)}(z) + (3-s)(1+z)^3 \left[1 - \overline{\Omega}^{(m)}(z) \right]}, \quad (4.24)$$

with

$$\overline{\Omega}^{(m)}(z) \equiv \lim_{s \rightarrow 0} \Omega_{\text{eff}}^{(m)}(z) = \frac{\Omega_0^{(m)} (1+z)^3}{1 + \Omega_0^{(m)} \left[(1+z)^3 - 1 \right]}. \quad (4.25)$$

Now, for the determination of the maximum numerical value s_{max} of the parameter s , using a comparative error analysis, we shall denote the statistical error on a given quantity Y in our model by δY , and that on the corresponding quantity \overline{Y} in the Λ CDM model by $\delta \overline{Y}$. As illustrated below, such an analysis requires taking into account a suitable model parameter which depends explicitly on s , and we also need to use the best fit value and the 68% confidence limit of the corresponding Λ CDM parameter for a given dataset. One may however note that the Λ CDM observational constraint on $\Omega_0^{(m)}$ (i.e. the 68% confidence limit $\delta \Omega_0^{(m)}$) would not serve the purpose, since by definition $\Omega_0^{(m)} = \Omega_{\text{eff}}^{(m)}(0) = \overline{\Omega}^{(m)}(0)$ is independent of s . To obtain s_{max} , let us therefore resort to the following:

Procedure 1: The error propagation equation corresponding to Eq. (4.23) is given by

$$\left(\frac{\delta \overline{H}_0}{\overline{H}_0} \right)^2 = \left(\frac{\delta H_0}{H_0} \right)^2 + \left(\frac{H_0}{\overline{H}_0} \right)^4 \left(\frac{\delta s}{6} \right)^2. \quad (4.26)$$

Let us stipulate $H_0 = \overline{H}_0 + \delta H_0$, and the minimum and maximum fractional error

$$\left| \frac{\delta H_0}{H_0} \right|_{\text{min}} = 0, \quad \text{and} \quad \left| \frac{\delta H_0}{H_0} \right|_{\text{max}} = \Delta_h \equiv \frac{|\delta \overline{H}_0|}{\overline{H}_0}. \quad (4.27)$$

For a given dataset, taking \overline{H}_0 as the best fit Λ CDM Hubble constant, and $|\delta \overline{H}_0|$ as its 68% error limit, we have a *fixed* value assigned to Δ_h . It then follows from Eq. (4.26) that

$$\delta s = 6 \left(1 - \left| \frac{\delta H_0}{H_0} \right| \right)^2 \left(\Delta_h^2 - \left| \frac{\delta H_0}{H_0} \right|^2 \right)^{1/2}. \quad (4.28)$$

Under the above stipulation, the second factor has the least value equal to zero, which ensures $\delta s \geq 0$. Moreover, the parameter s being positive, its upper bound s_{\max} is given by the maximum value of δs , i.e.

$$s_{\max} = 6 \Delta_h (1 + \Delta_h^2) . \quad (4.29)$$

Procedure 2: Let us re-express the equation (4.23) as

$$\Omega_0^{(m)} \bar{h}^2 = \Omega_0^{(m)} h^2 \left(1 - \frac{s}{3}\right)^2 , \quad (4.30)$$

where $\bar{h} = \bar{H}_0/[100 \text{ Km s}^{-1} \text{ Mpc}^{-1}]$ and $h = H_0/[100 \text{ Km s}^{-1} \text{ Mpc}^{-1}]$ are the reduced Hubble constants. We have the corresponding error propagation equation

$$\left[\frac{\delta(\Omega_0^{(m)} \bar{h}^2)}{\Omega_0^{(m)} \bar{h}^2} \right]^2 = \left[\frac{\delta(\Omega_0^{(m)} h^2)}{\Omega_0^{(m)} h^2} \right]^2 + \frac{(\Omega_0^{(m)} h^2)^2}{(\Omega_0^{(m)} \bar{h}^2)^2} \left(\frac{\delta s}{3} \right)^2 . \quad (4.31)$$

Stipulate now $\Omega_0^{(m)} h^2 = \Omega_0^{(m)} \bar{h}^2 + \delta(\Omega_0^{(m)} h^2)$, and the minimum and maximum fractional error

$$\left| \frac{\delta(\Omega_0^{(m)} h^2)}{\Omega_0^{(m)} h^2} \right|_{\min} = 0 , \quad \text{and} \quad \left| \frac{\delta(\Omega_0^{(m)} h^2)}{\Omega_0^{(m)} h^2} \right|_{\max} = \Delta_m \equiv \left| \frac{\delta(\Omega_0^{(m)} \bar{h}^2)}{\Omega_0^{(m)} \bar{h}^2} \right| . \quad (4.32)$$

with Δ_m kept fixed by taking $\Omega_0^{(m)} \bar{h}^2$ as the best fit value and $\delta(\Omega_0^{(m)} \bar{h}^2)$ the corresponding 68% margin for a given dataset. It follows that $\delta s \geq 0$, and working out the maximum value of δs one finds

$$s_{\max} = 3 \Delta_m . \quad (4.33)$$

A caveat is noticed though in the above ways of indirectly marginalizing the parameter s by using the Λ CDM parametric estimates: both \bar{H}_0 and $\Omega_0^{(m)} \bar{h}^2$ do not belong to the set of six independent parameters of the base Λ CDM model. We may in principle choose parameters other than \bar{H}_0 and $\Omega_0^{(m)} \bar{h}^2$ for the error analysis. However, none of such parameters would be among the basic six. This is evident from our compelling need to the use the equation (4.23) in the indirect determination of s_{\max} , by comparing with Λ CDM. Nevertheless, among the plausible parametric choices for performing the error analysis, preference may be given to $\Omega_0^{(m)} \bar{h}^2$ (used in the procedure 2 above). The reason is the simple (additive) relationship $\Omega_0^{(m)} = \Omega_0^{(b)} + \Omega_0^{(c)}$, where $\Omega_0^{(b)}$ and $\Omega_0^{(c)}$ are the present day values of the Λ CDM baryon density and cold dark matter (CDM) density parameters respectively. Since $\Omega_0^{(b)} \bar{h}^2$ and $\Omega_0^{(c)} \bar{h}^2$ are two of the six basic Λ CDM parameters, such simple relationship may lead to a low error limit on $\Omega_0^{(m)} \bar{h}^2$ (compared to that on \bar{H}_0 for instance, used in the procedure 1):

$$\left| \delta(\Omega_0^{(m)} \bar{h}^2) \right| = \sqrt{\left| \delta(\Omega_0^{(b)} \bar{h}^2) \right|^2 + \left| \delta(\Omega_0^{(c)} \bar{h}^2) \right|^2 + \left\langle \Omega_0^{(b)} \bar{h}^2, \Omega_0^{(c)} \bar{h}^2 \right\rangle} , \quad (4.34)$$

where $\left\langle \Omega_0^{(b)} \bar{h}^2, \Omega_0^{(c)} \bar{h}^2 \right\rangle$ is the 1σ error covariance of the base Λ CDM parameters $\Omega_0^{(b)} \bar{h}^2$ and $\Omega_0^{(c)} \bar{h}^2$. The smallness of $\left| \delta(\Omega_0^{(m)} \bar{h}^2) \right|$ does not however ensure that the corresponding percentage error Δ_m would be the least among those on all the other Λ CDM parameters suitable for the determination of s_{\max} using the comparative error analysis. In

fact, for the two procedures above, we mostly have $\Delta_m > \Delta_h$, as shown in Table 1. The s_{\max} values also shown therein, are obtained from Δ_h and Δ_m using Eqs. (4.29) and (4.33) respectively. All the values of Δ_h and Δ_m are computed using the Λ CDM parametric estimates from the following:

Dataset 1: WMAP 9 year data with the Baryon Acoustic Oscillation (BAO) and the Λ CDM Hubble constant \bar{H}_0 priors [7].

Dataset 2: WMAP 9 year data with BAO and \bar{H}_0 priors, combined with results of the Atacama Cosmology Telescope (ACT) [55], the South Pole Telescope (SPT) [56], and the Supernova Legacy Survey (SNLS) 3 year sample of high redshift supernovae of type 1a [57].

Dataset 3: PLANCK 2015 Cosmic Microwave Background (CMB) power spectra (TT, TE, EE) with polarization information from low multipole range temperature + polarization pixel-based likelihood (LowP) [8].

Dataset 4: PLANCK 2015 CMB power spectra (TT, TE, EE) and LowP, combined with weak lensing data (Lensing) [58] and external data (Ext) that includes the BAO and \bar{H}_0 priors and the Joint Lightcurve Analysis (JLA) sample [6] constructed from the SNLS [57] and the Sloan Digital Sky Survey (SDSS) [59] data, and many low redshift type-1a supernovae samples.

Observational datasets	Λ CDM parameters		Fractional error estimates	Upper bound on s	
	Best Fit values	68% limits		⁽¹⁾ $s_{\max}(\Delta_h)$	⁽²⁾ $s_{\max}(\Delta_m)$
1. WMAP_9y +BAO+ \bar{H}_0	$\Omega_0^{(m)} = 0.2880$ $\bar{H}_0 = 69.33$ $\Omega_0^{(m)}\bar{h}^2 = 0.1383$	$ \delta\Omega_0^{(m)} = 0.0100$ $ \delta\bar{H}_0 = 0.88$ $ \delta(\Omega_0^{(m)}\bar{h}^2) = 0.0025$	$\Delta_h = 0.01269$ $\Delta_m = 0.01808$	0.07615	0.05424
2. WMAP_9y+SPT +ACT+SNLS_3y +BAO+ \bar{H}_0	$\Omega_0^{(m)} = 0.2835$ $\bar{H}_0 = 69.55$ $\Omega_0^{(m)}\bar{h}^2 = 0.1371$	$ \delta\Omega_0^{(m)} = 0.0094$ $ \delta\bar{H}_0 = 0.78$ $ \delta(\Omega_0^{(m)}\bar{h}^2) = 0.0019$	$\Delta_h = 0.01121$ $\Delta_m = 0.01386$	0.06727	0.04158
3. PLANCK_2015 TT,TE,EE+LowP	$\Omega_0^{(m)} = 0.3156$ $\bar{H}_0 = 67.27$ $\Omega_0^{(m)}\bar{h}^2 = 0.1427$	$ \delta\Omega_0^{(m)} = 0.0091$ $ \delta\bar{H}_0 = 0.66$ $ \delta(\Omega_0^{(m)}\bar{h}^2) = 0.0014$	$\Delta_h = 0.00981$ $\Delta_m = 0.00981$	0.05887	0.02943
4. PLANCK_2015 TT,TE,EE+LowP +Lensing+Ext	$\Omega_0^{(m)} = 0.3089$ $\bar{H}_0 = 67.74$ $\Omega_0^{(m)}\bar{h}^2 = 0.1417$	$ \delta\Omega_0^{(m)} = 0.0062$ $ \delta\bar{H}_0 = 0.46$ $ \delta(\Omega_0^{(m)}\bar{h}^2) = 0.00097$	$\Delta_h = 0.00679$ $\Delta_m = 0.00684$	0.04074	0.02052

Table 1: Observational estimates (best fit values and 68% confidence limits) of Λ CDM cosmological parameters used for obtaining the upper bound s_{\max} of the model parameter s in the Einstein frame. Values of s_{\max} for different datasets are shown in the last two columns, for calculations using the \bar{H}_0 limits (procedure 1) and the $\Omega_0^{(m)}\bar{h}^2$ limits (procedure 2).

Using the estimated s_{\max} values, one can work out the maximal effective deviations from the Λ CDM matter density parameter $\bar{\Omega}^{(m)}(z)$ and the DE EoS value ($= -1$):

$$\delta\Omega_{\text{eff}}^{(m)}(z) := \Omega_{\text{eff}}^{(m)}(z, s_{\max}) - \bar{\Omega}^{(m)}(z), \quad \text{and} \quad \delta w_X(z) := 1 + w_X(z, s_{\max}). \quad (4.35)$$

Following are the features we observe here for the Einstein frame DE evolution:

In the near past: The matter density deviation from Λ CDM, $\delta\Omega_{\text{eff}}^{(m)}(z)$, is negative but increases in magnitude with gradually diminishing rate as we go back in the past, up to say a redshift $z = 2.5$. The variations of $\delta\Omega_{\text{eff}}^{(m)}(z)$ for all the datasets are shown in Fig. 1, the plots in the left panel are for s_{\max} obtained via the procedure 1, whereas those in the right panel correspond to s_{\max} obtained via the procedure 2. We find that the greater the value of the estimated s_{\max} , the greater is the magnitude of $\delta\Omega_{\text{eff}}^{(m)}$ at a given $z (> 0)$. The DE EoS deviation from Λ CDM,

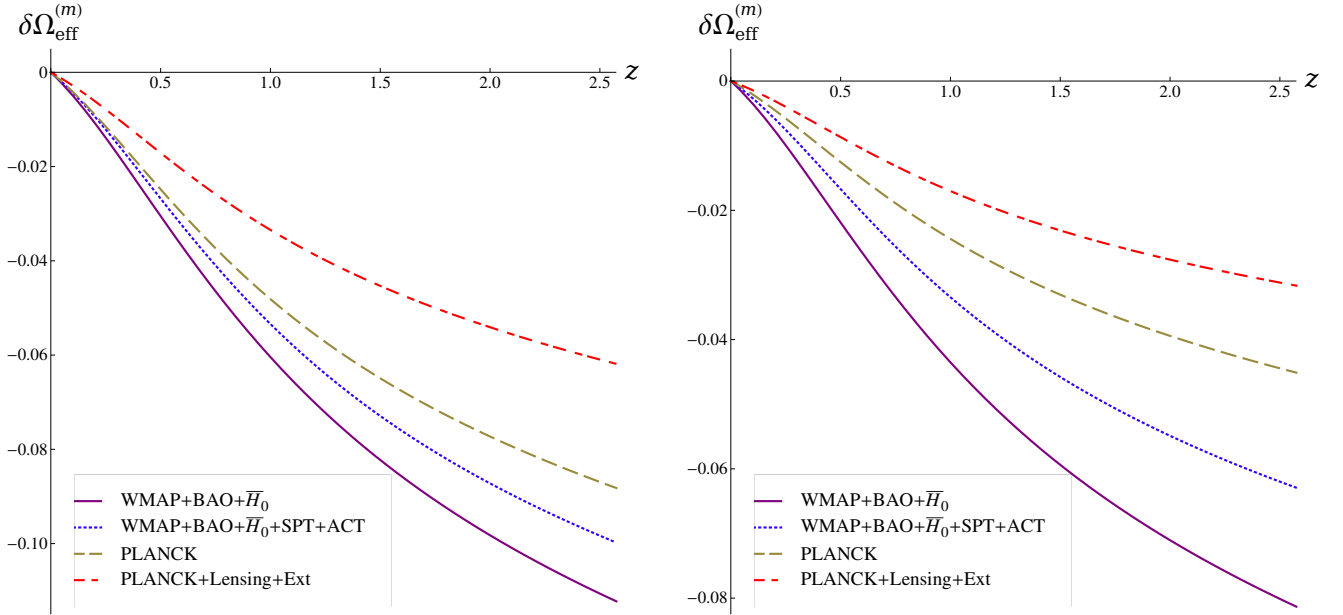


Figure 1: Variation (with redshift z) of $\delta\Omega_{\text{eff}}^{(m)}$, the Einstein frame maximal effective deviation from the Λ CDM matter density. The sets of curves in the left and right panels correspond to the sets of values of n_{\max} obtained using the procedures 1 and 2 respectively, for the various datasets.

$\delta w_X(z)$, on the other hand, remains positive at all redshifts $z > 0$, i.e. there is no revelation of an effective *phantom* regime ($w_X < -1$) in the near past. Fig. 2 exhibits the variations of $\delta w_X(z)$ for all the datasets, the plots in the left panel and in the right panel respectively correspond to s_{\max} obtained via the procedures 1 and 2. As we go back in the past (from $z = 0$, the present epoch), $\delta w_X(z)$ decreases initially and reaches a minimum value $\in [0.0056, 0.0254]$ at $z \in [0.3736, 0.3225]$, corresponding to $s_{\max} \in [0.02052, 0.07615]$ (obtained via the two procedures). Thereafter $\delta w_X(z)$ increases rapidly with z , till beginning to slow down around $z \simeq 2$. The greater the estimated s_{\max} , the greater is the value of $\delta w_X(z)$ at a given z . However, one can see an unevenness in the overall profile of the δw_X curves for the different s_{\max} values, which is to be attributed to the fact that δw_X depends not only on s_{\max} but also on the best fit value of $\Omega_0^{(m)}$.

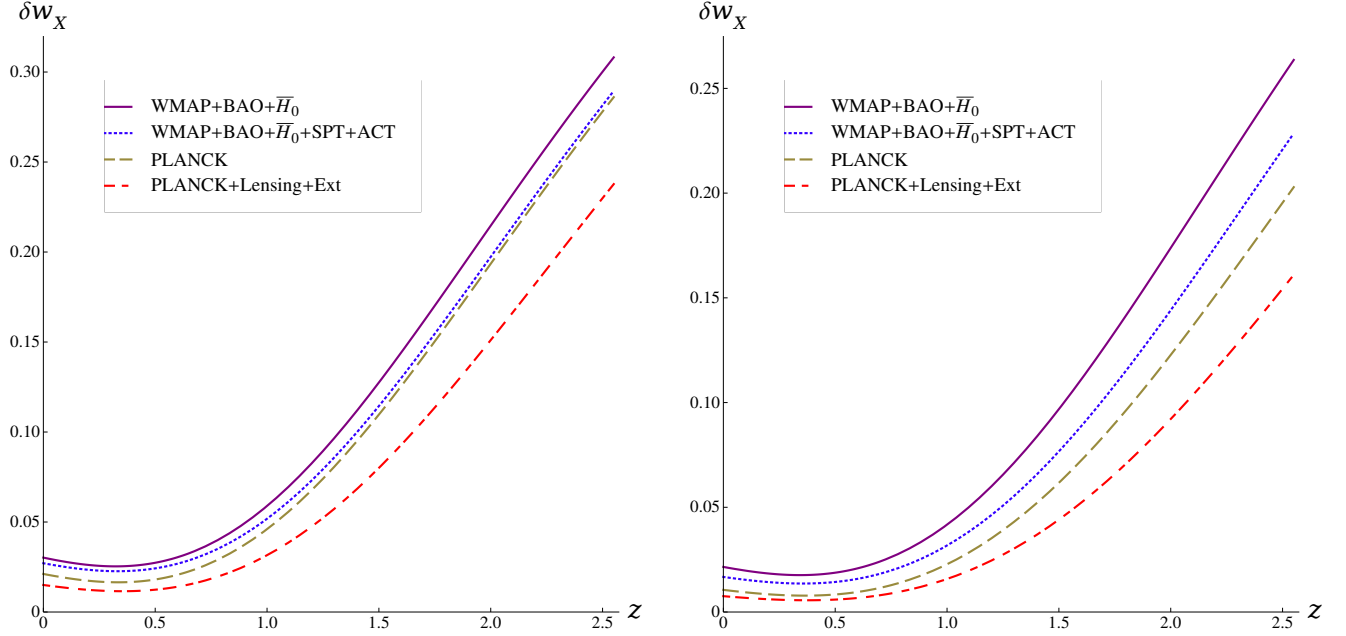


Figure 2: Variation (with redshift z) of δw_X , the Einstein frame maximal change over the Λ CDM dark energy EoS ($= -1$). The sets of curves in the left and right panels correspond to the sets of values of s_{\max} obtained using the procedures 1 and 2 respectively, for the various datasets.

Up to a moderately distant past: Let us now examine the DE evolution up to a fairly distant past (say from $z = 0$ to $z = 20$). As a reference s_{\max} value, we choose to take the largest estimate, viz. 0.07615 (obtained by the procedure 1, corresponding to the dataset 1). For this value of s_{\max} , the effective and the actual matter

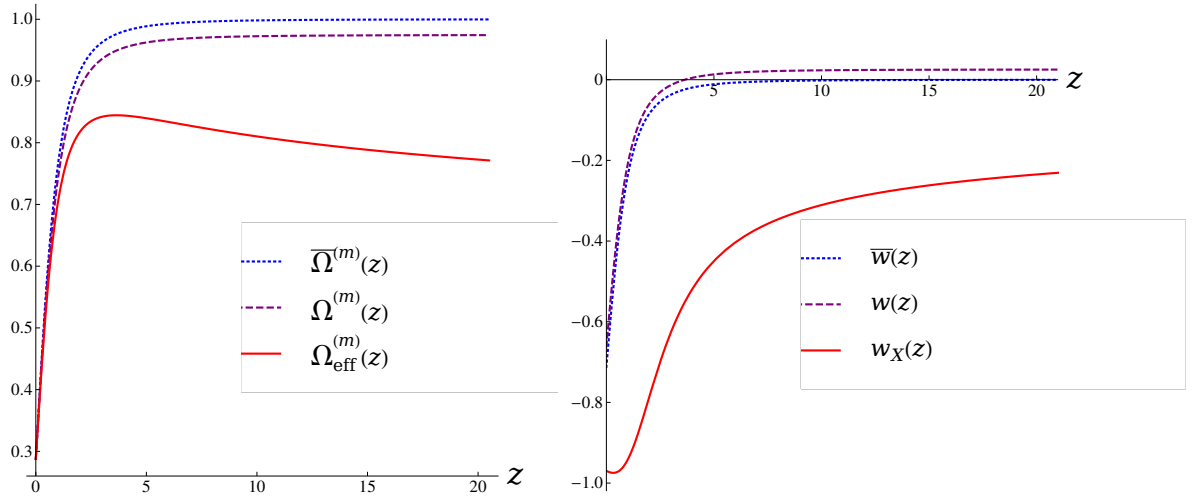


Figure 3: Einstein frame evolution upto a redshift $z = 20$, of (i) the matter density parameters $\Omega_{\text{eff}}^{(m)}(z)$, $\Omega^{(m)}(z)$, and $\bar{\Omega}^{(m)}(z)$ [in the *left panel*], and (ii) the EoS parameters $w_X(z)$, $w(z)$ and $\bar{w}(z)$ [in the *right panel*]. The value of s_{\max} used is the largest estimated one ($= 0.07615$ in Table 1).

density parameters, $\Omega_{\text{eff}}^{(m)}(z)$ and $\Omega^{(m)}(z)$ respectively, are shown in the left panel of Fig. 3, alongwith the Λ CDM matter density parameter $\bar{\Omega}^{(m)}(z)$. We see that the differences in the evolution pattern of all these quantities get

appreciable only at redshifts $z \gtrsim 1$. The evolution of $\Omega^{(m)}(z)$ is similar to that of $\bar{\Omega}^{(m)}(z)$ — increasing rapidly with z until saturating to a value close to 1 for $z \gtrsim 5$. The evolution pattern of $\Omega_{\text{eff}}^{(m)}(z)$ is different however — it increases rapidly from its value $\Omega_0^{(m)} = 0.288$ at $z = 0$, attains a maximum value 0.843 at $z = 3.6253$, and then decreases slowly with increasing z . The right panel of Fig. 3 shows the Einstein frame evolution of the effective DE EoS parameter $w_X(z)$ and the total EoS parameter $w(z)$ of the system (for $s_{\text{max}} = 0.07615$), alongwith the evolution of the Λ CDM total EoS parameter $\bar{w}(z)$. The evolution of $w(z)$ is found to be almost similar to that of $\bar{w}(z)$. However unlike the latter, $w(z)$ saturates to a value slightly greater than zero for $z \gtrsim 5$, implying no dust-like behaviour at high redshifts. This is expected, since in the Einstein frame the barotropic fluid is not typically the dust, but the one whose energy density varies as $(1+z)^{3+s}$ as a consequence of the scalar field interaction. The evolution pattern of $w_X(z)$ is altogether different however. At the present epoch we have $w_X(0) = -0.9698$, then w_X decreases with increasing z and attains a minimum value -0.9746 at $z = 0.3225$, turns around and increases rapidly to about -0.6 at $z \simeq 3$, and thereafter increases with z at a gradually diminishing rate. Most notably, $w_X(z)$ does not get saturated to a particular value till $z = 20$, and in fact keeps on increasing (albeit very slowly) even when z approaches its value at the *last scattering* (viz. $\simeq 1100$)⁸.

Near past to the extreme future: Finally, let us study the DE evolution from a redshift of near past (say $z = 1.5$) to the extreme future ($z = -1$). Once again we consider, for brevity, the largest estimated value of

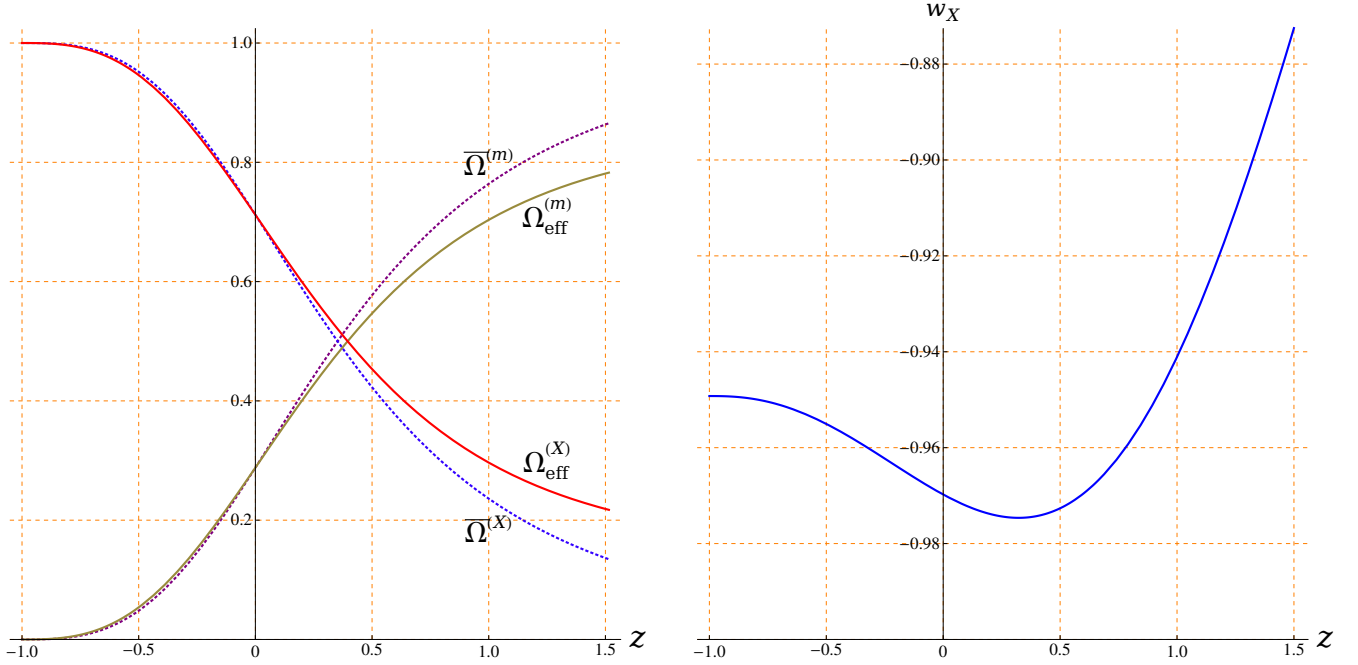


Figure 4: Einstein frame evolution from $z = 1.5$ to $z = -1$, of (i) the effective matter density and DE density parameters $\Omega_{\text{eff}}^{(m)}(z)$ and $\Omega_{\text{eff}}^{(X)}(z)$, alongwith the corresponding Λ CDM parameters $\bar{\Omega}^{(m)}(z)$ and $\bar{\Omega}^{(X)}(z)$ [in the *left panel*], and (ii) the DE EoS parameter $w_X(z)$ [in the *right panel*]. The value of s_{max} used is the largest estimate one ($= 0.07615$ in Table 1).

$s_{\text{max}} (= 0.07615)$. The left panel of Fig. 4 shows the evolutions of $\Omega_{\text{eff}}^{(m)}(z)$ and $\Omega_{\text{eff}}^{(X)}(z) = 1 - \Omega_{\text{eff}}^{(m)}(z)$, the effective density parameters for matter and the DE respectively. While in the entire future regime, $\Omega_{\text{eff}}^{(m)}(z)$ and $\Omega_{\text{eff}}^{(X)}(z)$ are

⁸Although this is not evident from Fig. 3, one may verify it by explicitly working out dw_X/dz from Eq. (4.14).

seen to be almost coincident to the corresponding Λ CDM density parameters $\bar{\Omega}^{(m)}(z)$ and $\bar{\Omega}^{(X)}(z) = 1 - \bar{\Omega}^{(m)}(z)$ respectively, their deviations from the latter become more and more significant as we go back in the past. The future evolutions are of course of the usual type, with the DE dominating over the barotropic matter, and asymptotically $\Omega_{\text{eff}}^{(m)} \rightarrow 0$ and $\Omega_{\text{eff}}^{(X)} \rightarrow 1$ as $z \rightarrow -1$. The redshift of the matter-DE equality ($\Omega_{\text{eff}}^{(m)} = \Omega_{\text{eff}}^{(X)} = 0.5$) for the dataset 1 considered here (corresponding to which $s_{\text{max}} = 0.07615$ by the procedure 1) turns out to be $z_{\text{eq}} = 0.3952$. This is not much different from that for Λ CDM, viz. $z_{\text{eq}} = 0.3521$, for the same dataset. We therefore only have a slight improvement from the Λ CDM model regarding the *coincidence* problem encountered in the latter. It can be checked easily that this is true not only for $s_{\text{max}} = 0.07615$ (corresponding to the dataset 1), but also for the other s_{max} values (corresponding to the other datasets) in Table 1. For $s_{\text{max}} = 0.07615$, the evolution of the effective DE EoS parameter $w_X(z)$ over the range $z \in [-1, 1.5]$ is shown in the right panel of Fig. 4. As z decreases from the value 1.5, we have w_X decreasing rapidly to a minimum value $w_X^{\text{min}} = -0.9746$ at $z = 0.3225$. Thereafter w_X increases (albeit rather slowly) as z decreases further. At the present epoch, $w_X(0) = -0.9698$, and in the future (i.e. for $z < 0$, or positive blueshifts), $w_X(z)$ continues to increase, until saturating to a value $\simeq -0.95$ at $z \simeq -0.8$. The overall evolution of $w_X(z)$ is smooth all the way to $z = -1$, with no discontinuities whatsoever.

4.4 Bounds on the torsion mode parameters and the effective Brans-Dicke parameter

Refer back to Eqs. (3.41) and (3.43) for the norms of the torsion mode vectors \mathcal{T}_μ and \mathcal{A}^μ respectively, with the assumption that the scalar field mass is solely due to the mode \mathcal{A}^μ . Using the Einstein frame solution ansatz (4.4), and the subsequent equation (4.8), we express these norms in terms of the Hubble rate H as

$$|\mathcal{T}|(z) = 3\kappa\sqrt{\beta}e^{\kappa\sqrt{\beta}\varphi(z)}\dot{\varphi}(z) = 3s(1+z)^{-s}H(z), \quad (4.36)$$

$$|\mathcal{A}| = 4\kappa\sqrt{3q\mathcal{U}_0} = 12(1+z)^{-s}H(z)\sqrt{q\left[1 - \frac{s}{3} - (1+z)^s\Omega_{\text{eff}}^{(m)}(z)\right]}, \quad (4.37)$$

with $q = 1, 2$ (respectively for the propositions 1 and 2 made in subsection 3.3). Let us denote the present-day value of the norm of \mathcal{T}_μ as $|\mathcal{T}|_0 \equiv |\mathcal{T}|_{z=0}$, the norm of \mathcal{A}^μ is of course fixed at all z . Our interest is in working out the bounds on $|\mathcal{T}|_0$ and $|\mathcal{A}|$ in terms of the independent parameters s_{max} , q , $\Omega_0^{(m)}$ and(or) the Λ CDM Hubble constant \bar{H}_0 [given by Eq. (4.23)]. Table 2 shows the upper limits:

$$\left[\frac{|\mathcal{T}|_0}{\bar{H}_0}\right]_{\text{max}} = 3s_{\text{max}}\left(1 - \frac{s_{\text{max}}}{3}\right)^{-1/2}, \quad \left[\frac{|\mathcal{A}|}{\bar{H}_0}\right]_{\text{max}} = 12\sqrt{q\left(1 - \Omega_0^{(m)}\right)}, \quad (4.38)$$

and

$$\left[\frac{|\mathcal{T}|_0}{|\mathcal{A}|}\right]_{\text{max}} = \frac{s_{\text{max}}}{4\sqrt{q}}\left(1 - \frac{s_{\text{max}}}{3} - \Omega_0^{(m)}\right)^{-1/2}, \quad (4.39)$$

computed using the best fit $\bar{H}_0, \Omega_0^{(m)}$ and the s_{max} estimates corresponding to the different datasets.

One may also note that while the upper bound s_{max} (obtained by the two procedures) has the range of values $\in [0.02052, 0.07615]$ for the various datasets considered, a fairly stringent restriction gets imposed on the effective BD parameter $\mathbf{w} = (s^{-1} - 3)/2$, viz. its minimum value $\mathbf{w}_{\text{min}} \in [5, 23]$ approximately (as shown in Table 2). This is fairly consistent (at least by the order of magnitude) with the lower bound $\mathbf{w}_{\text{min}} \simeq 40$, obtained in independent studies [45]. Further high values placed on \mathbf{w}_{min} [46] would imply $s \lesssim 10^{-2}$, which is perceptible as well, within the domain of validity of our parametric estimation from a comparative study with Λ CDM.

Observational datasets	$[\mathcal{T} _0/\overline{H}_0]_{\max}$	$[\mathcal{A} /\overline{H}_0]_{\max}$	$[\mathcal{T} _0/ \mathcal{A}]_{\max}$	\mathfrak{w}_{\min}
1. WMAP_9y+BAO+ \overline{H}_0	(1) 0.2314	(1) & (2) 10.1256 \sqrt{q}	(1) 0.0230/ \sqrt{q}	(1) 5.0660
	(2) 0.1642		(2) 0.0163/ \sqrt{q}	(2) 7.7183
2. WMAP_9y+SPT+ACT SNLS_3y+BAO+ \overline{H}_0	(1) 0.2041	(1) & (2) 10.1576 \sqrt{q}	(1) 0.0202/ \sqrt{q}	(1) 5.9327
	(2) 0.1256		(2) 0.0124/ \sqrt{q}	(2) 10.5250
3. PLANCK TT,TE,EE +LowP	(1) 0.1784	(1) & (2) 9.9274 \sqrt{q}	(1) 0.0181/ \sqrt{q}	(1) 6.9933
	(2) 0.0887		(2) 0.0089/ \sqrt{q}	(2) 15.4895
4. PLANCK TT,TE,EE +LowP+Lensing+Ext	(1) 0.1231	(1) & (2) 9.9759 \sqrt{q}	(1) 0.0124/ \sqrt{q}	(1) 10.7729
	(2) 0.0618		(2) 0.0062/ \sqrt{q}	(2) 22.8665

Table 2: Einstein frame upper bounds on the torsion mode parameters $|\mathcal{T}|$ and $|\mathcal{A}|$ (in units of \overline{H}_0), and their ratio, at the present epoch ($z = 0$). The two sets of values denoted by ⁽¹⁾ and ⁽²⁾ are due to the estimations using the procedures 1 and 2 respectively. The constant $q = 1, 2$ correspond to the two propositions in the subsection 3.3. For the different datasets, the respective minimum values of the effective Brans-Dicke parameter \mathfrak{w} are also shown.

5 MST Cosmology in the Jordan frame

Let us now consider, in this section, the Jordan frame to be suitable for interpreting the results of physical observations. We shall proceed along the lines of the previous section, presuming once again that the DE model emerging out of the MST theory is a slight modification of the Λ CDM model. Of course, while analyzing the Jordan frame action (3.15) (or more conveniently (3.19)) and the ensuing field equations, we encounter the running gravitational coupling constant, which is given explicitly by a function of the scalar field Φ [*cf.* Eq. (3.16)]. As such, the total energy-momentum tensor of matter and the scalar field combined, is not conserved. The matter Lagrangian though, being minimally coupled to gravity in the Jordan frame, renders the corresponding energy-momentum tensor $T_{\mu\nu}^{(m)}$ conserved [*cf.* Eq. (3.25)]. All these are quite unlike what we had in the Einstein frame. So the cosmology in the Jordan frame is expected to differ characteristically from that in the Einstein frame.

5.1 Cosmological equations and solution

The Jordan frame field equations (3.22), (3.23) and (3.26) lead to the Friedmann and Raychaudhuri equations

$$H^2(t) = \frac{1}{3\Phi(t)} \left[\rho^{(m)}(t) - 3H(t)\dot{\Phi}(t) + \frac{\mathfrak{w}\dot{\Phi}^2(t)}{2\Phi(t)} + \mathcal{V}(\Phi(t)) \right], \quad (5.1)$$

$$\dot{H}(t) = -\frac{1}{2\Phi(t)} \left[\rho^{(m)}(t) - H(t)\dot{\Phi}(t) + \frac{\mathfrak{w}\dot{\Phi}^2(t)}{\Phi(t)} + \ddot{\Phi}(t) \right], \quad (5.2)$$

where $H(t) := \dot{a}(t)/a(t)$ is now the Jordan frame Hubble parameter.

The conservation equation (3.25) yields the usual dust matter density

$$\rho^{(m)}(a) = \frac{\rho_0^{(m)}}{a^3}, \quad (5.3)$$

with its present-day value $\rho_0^{(m)} = \rho^{(m)}(t = t_0) = \rho^{(m)}(a = 1)$.

Assuming once again a simple power-law ansatz:

$$\Phi(a) = \Phi_0 a^n, \quad \text{with} \quad n = \text{a constant}, \quad (5.4)$$

we obtain

$$H^2(a) = \frac{\kappa^2}{3} \left(1 + n - \frac{\mathfrak{w}n^2}{6}\right)^{-1} \left[\frac{\rho_0^{(m)}}{a^{n+3}} + \mathcal{V}_0 \right], \quad (5.5)$$

$$[a^{2n+6} H^2(a)]' = \frac{2\kappa^2}{(2\mathfrak{w} + 3)n} \left[\rho_0^{(m)} a^{n+2} + 2\mathcal{V}_0 a^{2n+5} \right], \quad (5.6)$$

by recalling that $\mathcal{V}(\Phi) = \mathcal{V}_0 \Phi / \Phi_0$ [cf. Eq. (3.21)], with $\Phi_0 = \kappa^{-2}$.

It is easy to verify that for

$$n = \frac{1}{1 + \mathfrak{w}}, \quad (5.7)$$

the equations (5.5) and (5.6) are satisfied⁹, whence the Friedmann equation (5.5) reduces to

$$H^2(a) = \frac{2\kappa^2}{(n+2)(n+3)} \left[\frac{\rho_0^{(m)}}{a^{n+3}} + \mathcal{V}_0 \right]. \quad (5.8)$$

The validity condition for this, viz. $n > -2$, imposes the theoretical restriction $\mathfrak{w} > -3/2$. However, as has been the case in the Einstein frame, more stringent bounds on \mathfrak{w} could be obtained in the Jordan frame while matching the theoretical predictions with the observational results.

For convenience let us define the Jordan frame effective DE density ρ_X and DE pressure p_X as

$$\rho_X(a) := \frac{6}{(n+2)(n+3)} \left[\left\{ a^{-n} - 1 - \frac{n(n+5)}{6} \right\} \frac{\rho_0^{(m)}}{a^3} + \mathcal{V}_0 \right], \quad (5.9)$$

$$p_X(a) := \frac{6}{(n+2)(n+3)} \left[\frac{n\rho_0^{(m)}}{3a^{n+3}} - \mathcal{V}_0 \right], \quad (5.10)$$

so that the critical density of the universe is given by

$$\rho_C(a) := \frac{3H^2(a)}{\kappa^2} = \rho^{(m)}(a) + \rho_X(a), \quad (5.11)$$

which satisfies the conservation relation

$$\rho_C'(a) + \frac{3}{a} [\rho_C(a) + p_X(a)] = 0. \quad (5.12)$$

5.2 Effective cosmological parameters and their estimation

As a function of the redshift $z = (a^{-1} - 1)$, the matter density parameter is defined in the Jordan frame as

$$\Omega^{(m)}(z) := \frac{\rho^{(m)}(z)}{\rho_C(z)} = \Omega_0^{(m)} \frac{(1+z)^3}{\mathfrak{H}^2(z)}, \quad (5.13)$$

⁹There is also a solution $n = -2$. However, that would render $H^2 < 0$, unless it is stipulated that $(2\mathfrak{w} + 3) < 0$, i.e. the non-minimal parameter $\beta < 0$, a possibility which we discard for the reason mentioned earlier.

with $\Omega_0^{(m)} = \Omega^{(m)}(z=0)$, and the rationalized Hubble parameter $\mathfrak{H}(z)$ given by

$$\mathfrak{H}(z) \equiv \frac{H(z)}{H_0} = \left[1 + \frac{6\Omega_0^{(m)}}{(n+2)(n+3)} \left\{ (1+z)^{n+3} - 1 \right\} \right]^{1/2}, \quad (5.14)$$

where $H_0 \equiv H(z=0)$ is the Jordan frame Hubble constant.

The corresponding DE EoS parameter w_x is obtained as

$$w_x(z) := \frac{p_x(z)}{\rho_x(z)} = -1 + \frac{\Omega^{(m)}(z)}{1 - \Omega^{(m)}(z)} \left[\left(1 + \frac{n}{2}\right)^{-1} (1+z)^n - 1 \right], \quad (5.15)$$

and hence the EoS parameter of the system turns out to be

$$w(z) := \frac{p_x(z)}{\rho_c(z)} = -1 + \left(1 + \frac{n}{2}\right)^{-1} (1+z)^n \Omega^{(m)}(z). \quad (5.16)$$

It then follows that the requirement $w(0) < -1/3$ (for the presently accelerating universe) imposes the condition

$$n > 3\Omega_0^{(m)} - 2. \quad (5.17)$$

So the relation $n = (1 + \mathfrak{w})^{-1}$ implies *any one* of the following:

- (a) $\mathfrak{w} < \left[(3\Omega_0^{(m)} - 2)^{-1} - 1 \right]$, for either (i) $n > 0$ and $\Omega_0^{(m)} > 2/3$, or (ii) $n < 0$ and $\Omega_0^{(m)} < 2/3$,
- (b) $\mathfrak{w} > -1$, for (iii) $n > 0$ and $\Omega_0^{(m)} < 2/3$.

Now, we also have our earlier requirement $\mathfrak{w} > -3/2$. Therefore since $\Omega_0^{(m)} > 0$, it is easy to check that the condition (a) would hold only for $\Omega_0^{(m)} > 2/3$, i.e. for the case (i) above. This however implies an unusually large change over the concordance value (≈ 0.3) of the present-day matter density. As we are not considering our model to be drastically different from the widely favoured Λ CDM model, the condition (a) is unacceptable. So by the process of elimination we are left with the condition (b), i.e. $\mathfrak{w} > -1$, which approves $n > 0$ (the case (iii) above). Moreover, it should be pointed out that unlike the case in the Einstein frame, we are having here the constraint $\mathfrak{w} > -1$, tighter than the previous one ($\mathfrak{w} > -3/2$), regardless of any fiducial setting, such as $\Omega_0^{(m)} \simeq 0.3$.

As noticed in the Einstein frame, we see here that in the limit the model parameter $n \rightarrow 0$, the Λ CDM equations are recovered. For instance, the limit of Eq. (5.8) is the Λ CDM Friedmann equation, which in terms of the redshift z , and with $\Lambda \equiv \mathcal{V}_0$, is

$$\overline{H}^2(z) \equiv \lim_{s \rightarrow 0} H^2(z) = \frac{\kappa^2}{3} \left[\rho_0^{(m)} (1+z)^3 + \mathcal{V}_0 \right]. \quad (5.18)$$

Proceeding along the lines similar to that for the Einstein frame analysis in subsection 4.3, with every Λ CDM cosmological parameter denoted by an overbar $\{\overline{}\}$, we have here the following relationships between the Hubble constants:

$$\overline{H}_0 = H_0 \sqrt{\left(1 + \frac{n}{2}\right) \left(1 + \frac{n}{3}\right)}. \quad (5.19)$$

and between the matter density parameters:

$$\Omega^{(m)}(z) = \frac{(n+2)(n+3)(1+z)^3 \overline{\Omega}^{(m)}(z)}{\left[6(1+z)^{n+3} - n(n+5) \right] \overline{\Omega}^{(m)}(z) + (n+2)(n+3)(1+z)^3 \left[1 - \overline{\Omega}^{(m)}(z) \right]}, \quad (5.20)$$

with $\bar{\Omega}^{(m)}(z) \equiv \lim_{n \rightarrow 0} \Omega^{(m)}(z)$ given by Eq. (4.25).

Keeping all the other notations in subsection 4.3 unaltered, we obtain the maximum value of the model parameter (n here) to be

$$n_{\max} = \frac{12}{5} \Delta_h (1 + \Delta_h)^2, \quad (5.21)$$

by the procedure 1 (which uses the marginalized Λ CDM Hubble constant \bar{H}_0), and

$$n_{\max} = \frac{6}{5} \Delta_m (1 + \Delta_m), \quad (5.22)$$

by the procedure 2 (which uses the marginalized Λ CDM parameter $\Omega_0^{(m)} \bar{h}^2$). For the datasets 1-4 (the ones

Observational datasets	Λ CDM parameters		Fractional error estimates	Upper bound on n	
	Best Fit values	68% limits		⁽¹⁾ $n_{\max}(\Delta_h)$	⁽²⁾ $n_{\max}(\Delta_m)$
1. WMAP_9y +BAO+ \bar{H}_0	$\Omega_0^{(m)} = 0.2880$ $\bar{H}_0 = 69.33$ $\Omega_0^{(m)} \bar{h}^2 = 0.1383$	$ \delta\Omega_0^{(m)} = 0.0100$ $ \delta\bar{H}_0 = 0.88$ $ \delta(\Omega_0^{(m)} \bar{h}^2) = 0.0025$	$\Delta_h = 0.01269$ $\Delta_m = 0.01808$	0.03123	0.02209
2. WMAP_9y+SPT +ACT+SNLS_3y +BAO+ \bar{H}_0	$\Omega_0^{(m)} = 0.2835$ $\bar{H}_0 = 69.55$ $\Omega_0^{(m)} \bar{h}^2 = 0.1371$	$ \delta\Omega_0^{(m)} = 0.0094$ $ \delta\bar{H}_0 = 0.78$ $ \delta(\Omega_0^{(m)} \bar{h}^2) = 0.0019$	$\Delta_h = 0.01121$ $\Delta_m = 0.01386$	0.02751	0.01686
3. PLANCK_2015 TT,TE,EE+LowP	$\Omega_0^{(m)} = 0.3156$ $\bar{H}_0 = 67.27$ $\Omega_0^{(m)} \bar{h}^2 = 0.1427$	$ \delta\Omega_0^{(m)} = 0.0091$ $ \delta\bar{H}_0 = 0.66$ $ \delta(\Omega_0^{(m)} \bar{h}^2) = 0.0014$	$\Delta_h = 0.00981$ $\Delta_m = 0.00981$	0.02401	0.01189
4. PLANCK_2015 TT,TE,EE+LowP +Lensing+Ext	$\Omega_0^{(m)} = 0.3089$ $\bar{H}_0 = 67.74$ $\Omega_0^{(m)} \bar{h}^2 = 0.1417$	$ \delta\Omega_0^{(m)} = 0.0062$ $ \delta\bar{H}_0 = 0.46$ $ \delta(\Omega_0^{(m)} \bar{h}^2) = 0.00097$	$\Delta_h = 0.00679$ $\Delta_m = 0.00684$	0.01652	0.00826

Table 3: Observational estimates (best fit values and 68% confidence limits) of Λ CDM cosmological parameters used for obtaining the upper bound n_{\max} of the model parameter n in the Jordan frame. Values of n_{\max} for different datasets are shown in the last two columns, for calculations using the \bar{H}_0 limits (procedure 1) and the $\Omega_0^{(m)} \bar{h}^2$ limits (procedure 2).

considered in subsection 4.3), the calculated values of n_{\max} , via both the procedures, are shown in Table 3. With these n_{\max} values, we work out the effective maximal changes over the Λ CDM matter density parameter $\bar{\Omega}^{(m)}(z)$ and the Λ CDM DE EoS value ($= -1$), which are defined respectively as

$$\delta\Omega^{(m)}(z) := \Omega^{(m)}(z, n_{\max}) - \bar{\Omega}^{(m)}(z), \quad \text{and} \quad \delta\mathbf{w}_X(z) := 1 + \mathbf{w}_X(z, n_{\max}). \quad (5.23)$$

Following are the features of the Jordan frame DE evolution:

In the near past: Let us refer to Fig. 5, which shows the variations of $\delta\Omega^{(m)}(z)$ in the redshift range $z \in [0, 2]$ for all the datasets, with the plots in the left and right panels corresponding to the n_{\max} values obtained via the procedures 1 and 2 respectively. Unlike the characteristics of the analogous quantity $\delta\Omega_{\text{eff}}^{(m)}(z)$ in the Einstein frame, here we

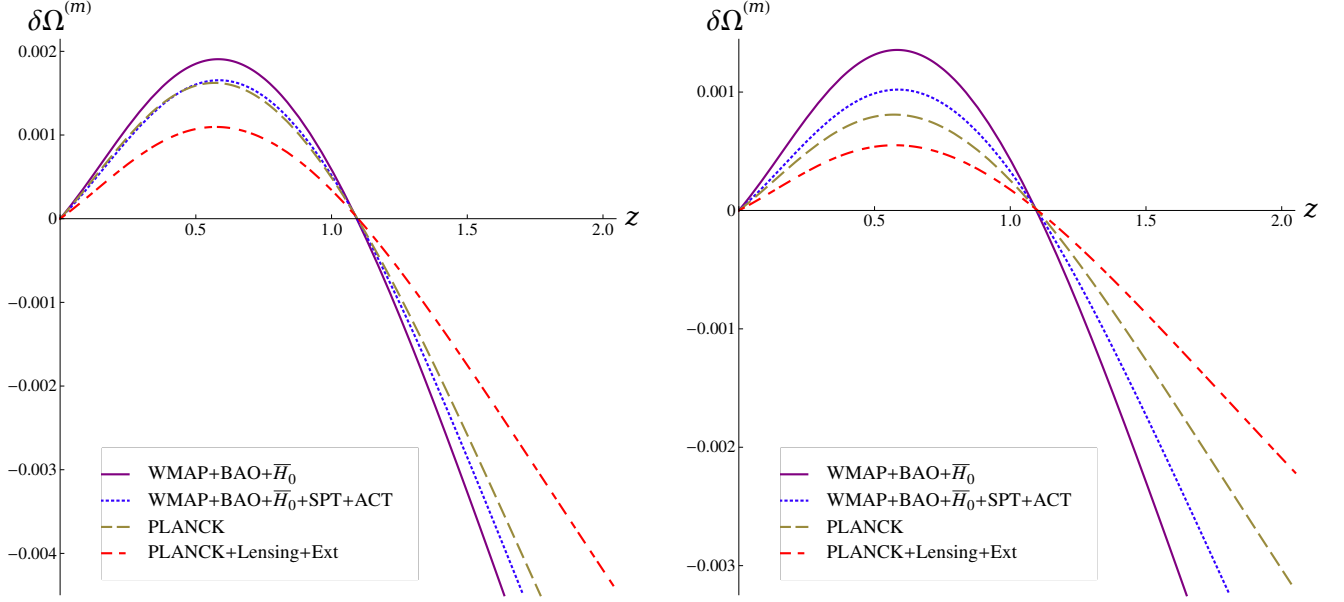


Figure 5: Variation (with redshift z) of $\delta\Omega^{(m)}$, the Jordan frame maximal deviation from the Λ CDM matter density. The sets of curves in the left and right panels correspond to the sets of values of n_{\max} obtained using the procedures 1 and 2 respectively, for the various datasets.

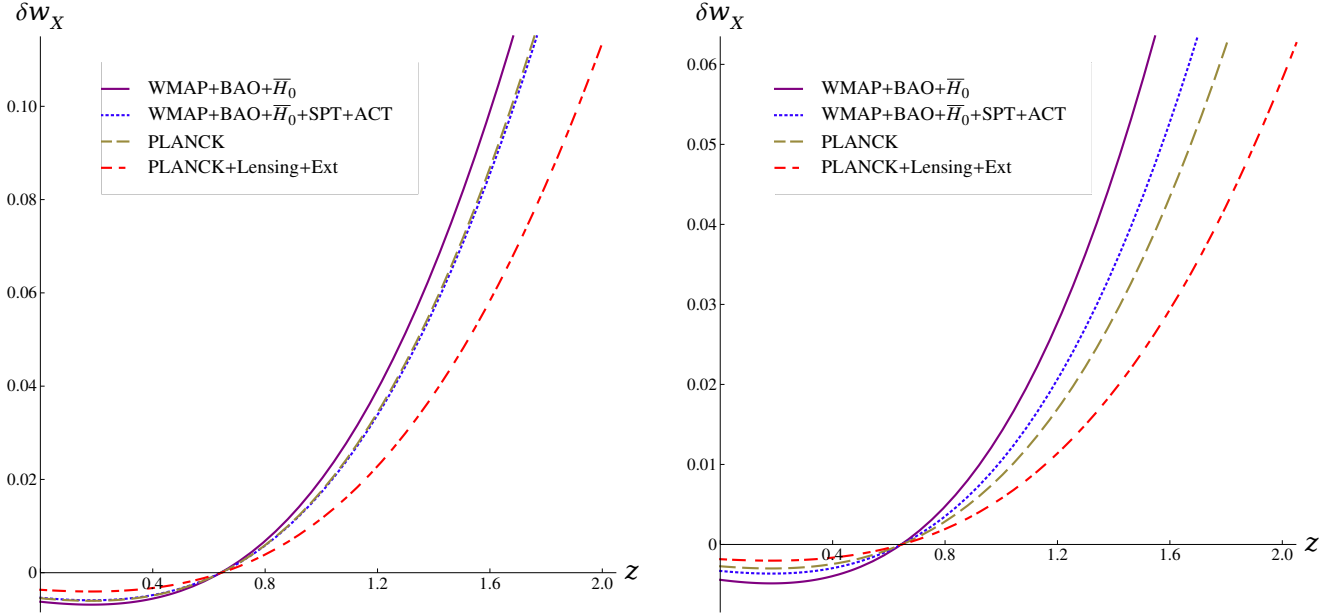


Figure 6: Variation (with redshift z) of δw_x , the Jordan frame maximal change over the Λ CDM dark energy EoS ($= -1$). The sets of curves in the left and right panels correspond to the sets of values of n_{\max} obtained using the procedures 1 and 2 respectively, for the various datasets.

see that $\delta\Omega^{(m)}(z) > 0$ initially, and grows with z as we go back in the past, reaches a maximum and then drops back to zero, and finally becomes negative with rapidly increasing magnitude as z increases further. Although the $\delta\Omega^{(m)}(z)$ curves are quite different for the different n_{\max} values (determined by the two procedures), the redshifts of the maximum point and the zero point change very little ($z \in [0.5693, 0.5865]$ and $z \in [1.0927, 1.1010]$ respectively)

for those n_{\max} values. Fig. 6 shows the variations of $\delta w_X(z)$ in the redshift range $z \in [0, 2]$ for all the datasets, with the left and right panel plots corresponding to n_{\max} determined by the procedures 1 and 2 respectively. The striking feature noticed here, in comparison to the (Einstein frame) plots in Fig. 2, is that $\delta w_X < 0$ (i.e. $w_X < -1$) at the present epoch ($z = 0$). That is, *presently the universe is undergoing an effective **super-accelerating** or **phantom** phase of expansion*. In the past, as z decreases (from say, a value equal to 2), $\delta w_X(z)$ changes from positive to negative (i.e. crosses over to the phantom phase), and attains a minimum (negative) value close to the present epoch, and increases slowly thereafter (but remains negative). The redshifts of both the crossing point ($z_c \simeq 0.64$) and the minimum point ($z \simeq 0.18$) are nearly irrespective of the value of n_{\max} . However, the minimum value of δw_X is larger in magnitude for larger n_{\max} . There is an unevenness in the overall profile of the $\delta w_X(z)$ curves for the different n_{\max} values, similar to what we have seen in the Einstein frame (for different s_{\max} therein). This can again be attributed to the dependence of δw_X on the best fit value of $\Omega_0^{(m)}$.

Up to a moderately distant past: For a fairly large redshift range $z \in [0, 20]$, we have the evolution of the matter density parameters $\Omega^{(m)}(z)$ and $\bar{\Omega}^{(m)}(z)$ as shown in the left panel of Fig. 3, and that of the EoS parameters $w_X(z)$, $w(z)$ and $\bar{w}(z)$ shown in the right panel of Fig. 3. As before, we take as the reference value of the model

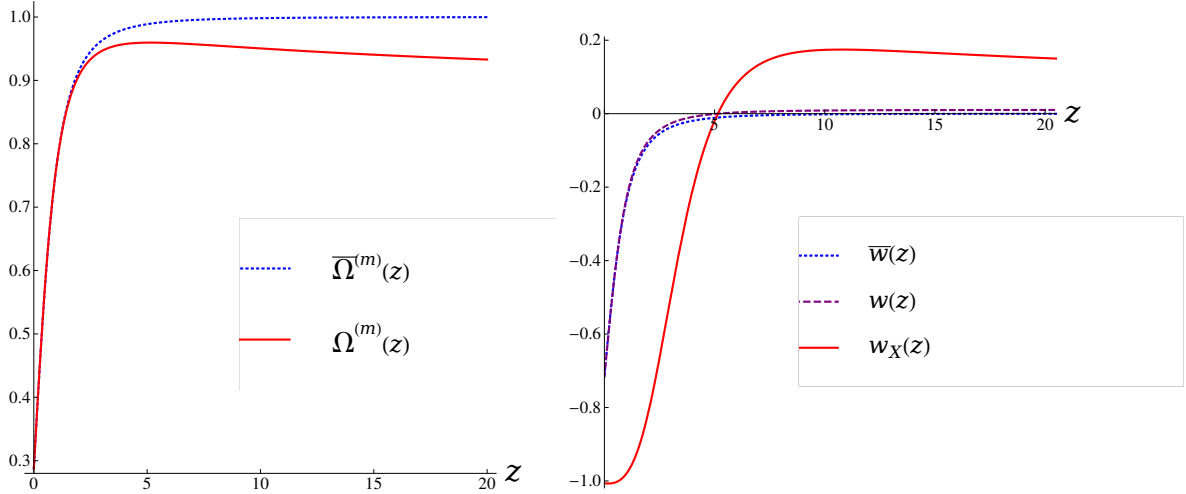


Figure 7: [Left panel] Jordan frame evolution of the matter density parameter $\Omega^{(m)}(z)$ compared with that for the Λ CDM model, viz. $\bar{\Omega}^{(m)}(z)$. [Right panel] Jordan frame evolution of the DE EoS parameter and the total EoS parameter, $w_X(z)$ and $w(z)$ respectively, compared with the Λ CDM total EoS parameter $\bar{w}(z)$. The curves stretch upto a fairly high redshift ($z = 20$), and correspond to the largest estimate of n_{\max} (viz. 0.03165, obtained by the procedure 1, from the WMAP dataset).

parameter, the largest estimated one, viz. $n_{\max} = 0.03123$, obtained via the procedure 1 applied to the dataset 1 (see Table 3). The $\Omega^{(m)}(z)$, $w_X(z)$ and $w(z)$ plots in Fig. 7 correspond to this value of n_{\max} . We see that $\Omega^{(m)}$ changes very little over $\bar{\Omega}^{(m)}$ up to $z \simeq 2$, and their difference starts to become more and more significant as we go back in the past (i.e. z increases) therefrom. Whereas $\bar{\Omega}^{(m)}$ gets saturated to unity at redshifts $z \gtrsim 5$, $\Omega^{(m)}$ attains a maximum value 0.9596 at $z = 5.1503$, and then falls off slowly with increasing z . Looking at the evolution of the total EoS parameter, we find that w remains almost identical to \bar{w} over the entire range $z \in [0, 20]$. The DE EoS parameter w_X , on the other hand, shows some interesting characteristics, in contrast to the fixed Λ CDM value ($= -1$) and also the Einstein frame w_X (whose evolution is shown in Fig. 3). Here we find that $w_X = -1.0062$ at

the present epoch ($z = 0$), and as we go back in the past, w_X drops to a minimum value -1.0069 at $z = 0.1815$, turns back and crosses the Λ CDM value ($= -1$) at $z_c = 0.6424$, continues increasing rapidly with z until slowing down at $z \simeq 4$, crossing the zero value at $z = 5.1503$ and increasing further till attaining a maximum value 0.1745 at $z = 10.7731$, turning back once again finally and decreasing very slowly with further increase in z .

Near past to the extreme future: Finally, let us refer to the Fig. 8 for the parametric evolution from a redshift of near past to that at the extreme future ($z = -1$), with the reference value $n_{\max} = 0.03123$. The curves in the left

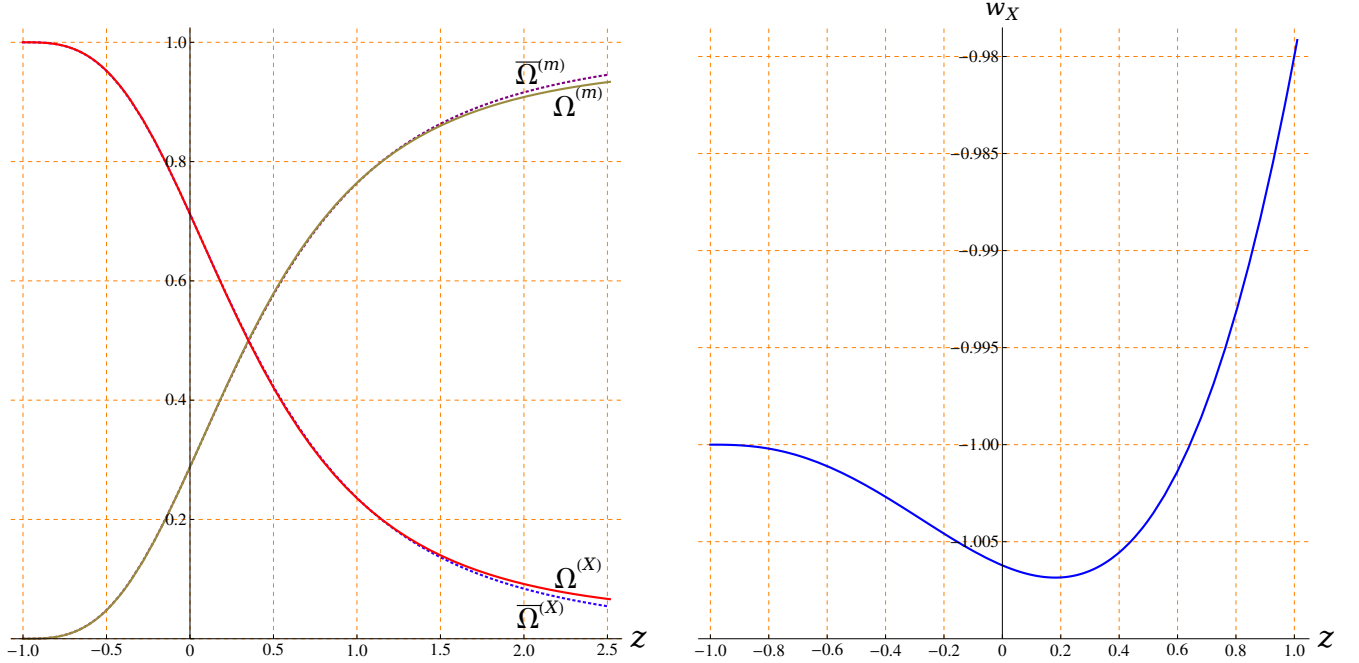


Figure 8: Jordan frame evolution of the density parameters for matter and DE, $\Omega^{(m)}(z)$ and $\Omega^{(X)}(z)$ respectively, compared with those (viz. $\bar{\Omega}^{(m)}(z)$ and $\bar{\Omega}^{(X)}(z)$ for the Λ CDM model (in the left panel), and that of the DE EoS parameter $w_X(z)$ (in the right panel). All the curves are for the largest estimated value of $n_{\max} (= 0.03123)$, and depict the variation of the corresponding quantities from the near past ($z = 2.5$ or 1.5) to the absolute future ($z = -1$).

panel show the comparison of the density parameters $\Omega^{(m)}(z)$ and $\Omega^{(X)}(z) = 1 - \Omega^{(m)}(z)$, for matter and the DE respectively, with the corresponding ones Λ CDM ones, $\bar{\Omega}^{(m)}(z)$ and $\bar{\Omega}^{(X)}(z)$. We observe that there is no significant deviation of $\Omega^{(m)}$ from $\bar{\Omega}^{(m)}$, and that of $\Omega^{(X)}$ from $\bar{\Omega}^{(X)}$, until a z has a fairly high value ($\gtrsim 1.75$), far from that at the matter-DE equality point $z_{eq} = 0.3495$ (which is almost coincident with $z_{eq} = 0.3522$ for Λ CDM). So we can safely say that the status of the coincidence problem in the Λ CDM model is unchanged in our Jordan frame analysis. The same could be inferred as well for the other datasets and the corresponding n_{\max} values, as can be checked explicitly. The right panel of Fig. 8 the evolution of the DE EoS parameter w_X (for $n_{\max} = 0.03123$) in the range $z \in [-1, 1]$. The pattern of this evolution is similar to that of w_X in the Einstein frame (refer back to Fig. 4). However, the most striking change here is the effective phantom regime, which is not *transient*. With decreasing z , w_X decreases and crosses the phantom barrier at $z_c = 0.6424$, continues to decrease till reaching the minimum value $w_X^{\min} = -1.0069$ at $z = 0.1815$, turns back and increases, but always remains below -1 . Only asymptotically, $w_X \rightarrow -1$ (from below) as $z \rightarrow -1$.

5.3 Bounds on the torsion mode parameters and the effective Brans-Dicke parameter

The Jordan frame solution ansatz (5.4) and the Friedmann equation (5.8) lets one to express the norms of the torsion mode vectors \mathcal{T}_μ and \mathcal{A}^μ , given by Eqs. (3.39) and (3.43), in terms of the Hubble rate H as

$$|\mathcal{T}|(z) = \frac{3\dot{\Phi}(z)}{2\Phi(z)} = \frac{3n}{2} H(z), \quad (5.24)$$

$$|\mathcal{A}| = 4\kappa\sqrt{3q\mathcal{V}_0} = 2H(z)\sqrt{6q\left[(n+2)(n+3) - 6(1+z)^n\Omega_{\text{eff}}^{(m)}(z)\right]}, \quad (5.25)$$

where $q = 1, 2$ correspond to the propositions 1 and 2 made in the subsection 3.3, and we are assuming that the mode \mathcal{A}^μ is responsible entirely for the scalar field mass. Table 4 shows the present-day trace mode norm $|\mathcal{T}|_0 \equiv |\mathcal{T}|_{z=0}$,

Observational datasets	$[\mathcal{T} _0/\overline{H}_0]_{n_{\text{max}}}$	$[\mathcal{T} _0/ \mathcal{A}]_{n_{\text{max}}}$	\mathbf{w}_{min}
1. WMAP_9y+BAO+ \overline{H}_0	(1) 0.0462	(1) $0.0045/\sqrt{q}$	(1) 31.0205
	(2) 0.0328	(2) $0.0032/\sqrt{q}$	(2) 44.2694
2. WMAP_9y+SPT+ACT SNLS_3y+BAO+ \overline{H}_0	(1) 0.0408	(1) $0.0040/\sqrt{q}$	(1) 35.3504
	(2) 0.0251	(2) $0.0025/\sqrt{q}$	(2) 58.3120
3. PLANCK TT,TE,EE +LowP	(1) 0.0357	(1) $0.0036/\sqrt{q}$	(1) 40.6493
	(2) 0.0177	(2) $0.0018/\sqrt{q}$	(2) 83.1043
4. PLANCK TT,TE,EE +LowP+Lensing+Ext	(1) 0.0246	(1) $0.0025/\sqrt{q}$	(1) 59.5327
	(2) 0.0123	(2) $0.0012/\sqrt{q}$	(2) 120.0654

Table 4: Torsion trace mode parameter at the present epoch, $|\mathcal{T}|_0$, in units of the Λ CDM Hubble constant \overline{H}_0 , and the torsion pseudo-trace mode parameter $|\mathcal{A}|$, in the Jordan frame. The sets of values denoted by ⁽¹⁾ and ⁽²⁾ correspond to the estimations using the procedures 1 and 2 respectively. The constant $q = 1, 2$ correspond to the two propositions in the subsection 3.3. For the different datasets, the respective minimum values of the effective Brans-Dicke parameter \mathbf{w} are also shown.

in units of the Λ CDM Hubble constant \overline{H}_0 and $|\mathcal{A}|$, evaluated at $n = n_{\text{max}}$:

$$\left[\frac{|\mathcal{T}|_0}{\overline{H}_0}\right]_{n_{\text{max}}} = \frac{3\sqrt{3}n_{\text{max}}}{\sqrt{2(n_{\text{max}}+2)(n_{\text{max}}+3)}}, \quad \text{and} \quad (5.26)$$

$$\left[\frac{|\mathcal{T}|_0}{|\mathcal{A}|}\right]_{n_{\text{max}}} = \frac{\sqrt{3}n_{\text{max}}}{4\sqrt{2q\left[(n_{\text{max}}+2)(n_{\text{max}}+3) - 6\Omega_0^{(m)}\right]}}, \quad (5.27)$$

using the best fit \overline{H}_0 , $\Omega_0^{(m)}$ and the n_{max} estimates (by the procedures 1 and 2), for the different datasets. Also shown in Table 4, the corresponding values of the lower bound on the effective BD parameter $\mathbf{w} = (n^{-1} - 1)$. These values are in the range $\mathbf{w}_{\text{min}} \in [31, 120]$ approximately. So, compared to what obtained in the Einstein frame (see Table 2 in subsection 4.4), we have the values of \mathbf{w}_{min} here to be more in agreement with those found in independent studies [45, 46].

6 Transformations relating parameters in the two frames

So far we have dealt with the observational aspects of the DE model that emerges out of the MST equivalent scalar-tensor theory, assuming *any one* of the Einstein and the Jordan frames to be of physical relevance. We have obtained the field equations in the two frames and considered them to be describing the dynamical evolution of the universe in respective circumstances. Explicit solutions of such equations enabled us to estimate the model parameters which quantify the state of cosmology at any given epoch. However, the question that remains is that if the solutions in one frame, say the Jordan frame, are known, can we deduce the corresponding solutions in the other (Einstein) frame without having to go through the tedious process of explicitly solving the field equations in that frame. We can indeed do that, but only with the knowledge of how the cosmic time, the scale factor and the scalar field and torsion parameters transform from one frame to the other. Such transformations could be fixed by the relations (3.27) and (3.29). The metric redefinition (in terms of the conformal factor) yields two independent equations which, in view of preserving the FRW metric structure (3.1), defines the cosmic time and the scale factor in a transformed frame. For the ansatzé chosen in the two frames, viz. Eqs. (4.4 and (5.4), the transformation equations are given by

$$\hat{t} = \int dt a^{n/2}(t) , \quad \hat{a}(\hat{t}) = a^{(n+2)/2}(t) . \quad (6.1)$$

In addition, one may verify that

$$s = \frac{n}{n+2} . \quad (6.2)$$

Note again that the Einstein frame quantities are marked with a (\wedge) over them. Given an expression in one frame, the use of the above equations would lead to the corresponding expression in the other frame. The estimated upper bounds on the numerical values of the parameters s and n , shown respectively in the Tables 1 and 3, do not however comply with Eq. (6.2). This is expected, since such estimates have been made assuming either the Einstein frame or the Jordan frame as the physical frame in the respective analysis. This facilitated the use of the same observational data for computing the fractional errors Δ_h and Δ_m in each of the frames. The idea behind our approach in sections 4 and 5 has therefore been to differentiate between the physical viability of the two frames using the computed results. One could have taken the alternative route of appropriately scaling the observational data using the above transformation equations, considering the Einstein and the Jordan frames to be physically equivalent. However, that would inevitably have lead back to the longstanding problem of dealing with the running coupling constants in a physical theory.

7 Conclusion

We have thus demonstrated that a non-minimal metric-scalar coupling with space-time torsion may lead to a self-consistent DE model with slow dynamics. The latter of course complies with the requirement of not having much parametric distortion from the base Λ CDM model. Such a requirement arizes naturally in view of (i) the wide observational support of Λ CDM (despite its theoretical limitations), and (ii) the miniscule experimental signature of torsion in extensive researches till date. Moreover, one has to get in an agreement with the high value of the lower bound on the effective Brans-Dicke parameter \mathfrak{w} in the MST equivalent scalar-tensor theory. Our analysis

in sections 4 and 5 show that such a bound is indeed tenable in our non-minimal MST formalism in the standard cosmological setup. While the non-minimal coupling removes the ambiguity in choosing the MST action, one has to take into account the constraints on the torsion mode parameters for maintaining the FRW metric structure. The result of course, is that the trace mode of torsion is sourced by the scalar field, which leaves us with the arbitrariness only in selecting the potential for the scalar. As it turned out, for an almost Λ CDM like DE model, it suffices taking just a mass term for the scalar field. We have made propositions for such a scalar field mass (or, at least a part of it) out of torsion itself, in a way that the completely antisymmetric part of the latter gets eliminated via a suitably chosen constraint. Thus overall, the MST action gets reduced to the scalar-tensor form, alongwith the potential of the scalar field given by its mass term, and the cosmological matter as the non-relativistic dust. Now, a major obstacle in the scalar-tensor theory is to choose between the two frames, Einstein and Jordan, the “physical” one for interpreting the observational results. One may of course consider the two frames to be physically equivalent, provided in one of them the units of length, time and mass are explicit functions of the scalar field (and therefore time-varying) [44]. We have however discarded such a scenario (on account of its feasibility), and have also taken the non-minimal coupling parameter β to be positive definite (so as to ensure that the underlying quantum theory is bounded from below). Considering rigid sets of units in both the frames, our objective has been to carry out the analysis separately in the Einstein frame (supposing it to be the physical one), as well as in the Jordan frame (supposing it to be physical). This is of course a safeguard approach, in lieu of getting involved in the longstanding debate as to which frame is actually physical.

From the technical point of view, instead of performing a likelihood analysis, we have stipulated that the cosmological parameters for our model to be kept within the 68% confidence limits of the corresponding ones for a reference Λ CDM model. This enabled us a direct way of complying with the modern acceptance range of the present-day values of the cosmological parameters, via a reasonable order of magnitude estimation of the same. We have referred to two procedures of determining the statistical upper bound on our model parameter from the Λ CDM parametric marginalizations for a few recent datasets. Such procedures have been followed in both the Einstein frame and the Jordan frame analysis in sections 4 and 5 respectively. What we have observed is that, even with the small parametric changes, there are significant characteristic differences of our model with Λ CDM. Most notably, the effective EoS parameter w_x for dark energy in the Jordan frame crosses over from a value > -1 to a value < -1 in the near past. It then reaches a minimum value, turns back but continues to remain below -1 throughout the present and future evolution of the universe. Such a crossing is usually not tenable in the scalar field models of DE, e.g. quintessence or k-essence, unless there is(are) *ghost* or *phantom* degree(s) of freedom involved, which bring(s) in instabilities [61]. However, in our case we have the effective cross-over to the *phantom regime* in a Brans-Dicke equivalent theory, which is at least stable against cosmological density perturbations [44, 62]. So unlike most of the scalar field DE formulations, our MST cosmological setup in the Jordan frame does not pre-assign a theoretical limitation for the statistical marginalization of the cosmological parameters using the observational data. Another important aspect is that in the model-independent parametrizations of DE, the phantom barrier crossing is actually favoured (albeit mildly) by the recent observational data. For example, the Planck 2015 (TT,TE,EE + LowP + Lensing + Ext) results [8] show that w_x given by the Chavellier-Polarsky-Linder (CPL) ansatz [60], has the best fit value at the present epoch $w_x(0) = -1.019$. One may check that estimations close to this value

would indeed be obtained from our analysis in section 5, for the same Planck data (i.e. the dataset 4 in Table 3), viz. $w_X(0) = -1.0037$ (corresponding to $n = n_{\max} = 0.01652$, by the procedure 1), and $w_X(0) = -1.0018$ (corresponding to $n = n_{\max} = 0.00826$, by the procedure 2).

Finally, we should emphasize the high minimal estimates (corresponding to the different datasets) of the effective Brans-Dicke parameter \mathfrak{w} , found in both the Einstein frame and the Jordan frame analysis in sections 4 and 5 (see Tables 2 and 4). Such high estimates are in agreement with the values obtained in many independent studies [45, 46], which are therefore in support of our MST-DE model. In fact, they also imply that the BD theory is not much of a deviation from GR. In our case, since we have the torsion field as one of key ingredients in the effective BD formulation, the high estimates of the lower limit of \mathfrak{w} simply mean that the direct effects of the torsion modes on the space-time geometry are very weak. Especially, for the late-time cosmologies, one always expects torsion to have a minor role. This is indeed reflected in the smallness of the upper limit on the present-day value of the torsion trace mode parameter shown in the Tables 2 and 4. So, the effective DE evolution in our MST formalism must majorly be attributed to the effect of the coupling of torsion with the scalar field, or more appropriately, that of the mass of the scalar, whether due to the torsion pseudo-trace or otherwise.

Some open questions are in order: (i) what about the mathematical stability of the above formalism, i.e. against small fluctuations in the solution space? (ii) what about the stability against density perturbations? (iii) what if the cosmological dust interacts in a very non-trivial way with torsion? (iv) what if we take some other cosmological fluid, e.g. Chaplygin gas, instead of dust? (v) what if choose to consider the non-minimal coupling in some other form, or assign a dynamical source to the torsion pseudo-trace (such as the Kalb-Ramond field)? Works addressing a few of these are underway [63, 64], which we hope to report soon.

Acknowledgement

SS acknowledges the R & D Grant DRCH/R & D/2013-14/4155, Research Council, University of Delhi. The work of ASB is supported by the Council of Scientific and Industrial Research (CSIR), Government of India.

References

- [1] A. G. Riess *et al.*, *Astron. J.* **116** 1009 (1998);
S. Perlmutter *et al.*, *Astrophys. J.* **517** 565 (1999).
- [2] K. Bamba *et al.*, *Astrophys. Space Sci.* **342** 155 (2012);
M. Li *et al.*, *Dark Energy*, World Scientific, Singapore (2014);
E. J. Copeland, M. Sami and S. Tsujikawa, *Int. J. Mod. Phys. D* **15** 1753 (2006);
G. Wolschin, *Lectures on Cosmology: Accelerated Expansion of the Universe*, Springer, Berlin, Heidelberg (2010)
L. Amendola and S. Tsujikawa, *Dark Energy: Theory and Observations*, Cambridge University Press, United Kingdom (2010)

- [3] S. M. Carroll, Living Rev. Rel. **4** 1 (2001);
T. Padmanabhan, Phys. Rept. **380** 235 (2006);
J. M. Cline, arXiv:hep-th/0612129;
J. Polchinski, arXiv:hep-th/0603249;
L. M. Krauss and R. J. Scherrer, Gen. Rel. Grav. **39** 1545 (2007).
- [4] S. Dodelson, Modern Cosmology, Academic Press, Elsevier (2003);
J. A. Peacock, Cosmological Physics, Cambridge University Press, United Kingdom (1999);
P. J. E. Peebles and B. Ratra, Rev. Mod. Phys. **75**, 559 (2003);
J. Sol, J. Phys. Conf. Ser. **453** 012015 (2013).
- [5] M. Kowalski *et al.*, Astrophys. J. **686** 749 (2008);
N. Suzuki *et al.*, Astrophys. J. **746** 85 (2012). arXiv:1105.3470
- [6] M. Betoule *et al.*, Improved cosmological constraints from a joint analysis of the SDSS-II and SNLS supernova samples. Astron. & Astrophys. **568** A22 (2014).
- [7] G. F. Hinshaw *et al.*, Nine-year Wilkinson Microwave Anisotropy Probe (WMAP) Observations: Cosmological Parameter Results, Astrophys. J. Suppl. **208** 19 (2013);
C. L. Bennett *et al.*, Nine-Year Wilkinson Microwave Anisotropy Probe (WMAP) Observations: Final Maps and Results, Astrophys. J. Suppl. **208** 20B (2013)
- [8] Planck 2015 results, XIII. “Cosmological parameters”, P.A.R Ade *et al.*, Astron. Astrophys **594** A13 (2016);
Planck 2015 results, XIV. “Dark energy and modified gravity”, P.A.R Ade *et al.*, Astron. Astrophys **594** A14 (2016).
- [9] M. Khurshudyan, E. Chubaryan and B. Pourhassan, Int. J. Theor. Phys. **53** 2370 (2014);
I. Zlatev, L. Wang and P.J. Steinhardt Phys. Rev. Lett. **82** 896 (1999);
S. Tsujikawa, Class. Quant. Grav. **30** 214003 (2013).
- [10] C. Armendariz-Picon, V. Mukhanov and P. J. Steinhardt Phys. Rev. **D 63** 103510 (2001);
M. Sharif, K. Yesmakhanova, S. Rani et al., Eur. Phys. J. **C 72** 2067 (2012);
S. Sur and S. Das, JCAP **0901** 007 (2009), and references therein.
- [11] F. Piazza and S. Tsujikawa, JCAP 0407 004 (2004);
K Karami and K Fahimi Class. Quant. Grav. **30**, 065018 (2013).

- [12] G. Calcagni and A. R. Liddle, *Phys. Rev. D* **74**, 043528 (2006);
 C.J.A.P. Martins and F.M.O. Moucherek, *Phys. Rev. D* **93**, 123524 (2016).
 J. S. Bagla, H. K. Jassal, and T. Padmanabhan, *Phys. Rev. D* **67**, 063504 (2003).
- [13] Benjamin Elder, Justin Khoury et al, *Phys. Rev. D* **94**, 044051 (2016);
 P. Brax and N. Tamanini, *Phys. Rev. D* **93** 103502 (2016), and references therein;
- [14] M. C. Bento, O. Bertolami, and A. A. Sen, *Phys. Rev. D* **66**, 043507 (2002);
 L. Xu, J. Lu and Y. Wang, *Eur. Phys. J. C* **72** 1883 (2012);
 L. Xu, Y. Wang and H. Noh, *Eur. Phys. J. C* **72** 1931 (2012).
- [15] E. Witten, *The Cosmological constant from the viewpoint of string theory*, 4th International Symposium on Sources and Detectors Conference, Berlin, Germany, Springer (2001);
 R. Bousso, *The Cosmological Constant Problem, Dark Energy, and the Landscape of String Theory*, *Pontif. Acad. Sci. Scr. Varia* **119** 129-151 (2011);
 G. Shiu and B. Greene, *Perspectives on String Phenomenology*, World Scientific, Singapore (2015).
- [16] C. Ahn, C. Kim, and E. V. Linder, *Phys. Rev. D* **80**, 123016 (2009);
 M. R. Garousi, M. Sami and Shinji Tsujikawa, *Phys. Rev. D* **71**, 083005 (2005);
 J. Martin and M. Yamaguchi, *Phys. Rev. D* **77**, 123508 (2008);
 S. Sur, arXiv: 0902.1186 [astro-ph.CO].
- [17] B. Jain et al., *ApJ* **779** 39 (2013);
 T. Clifton et al., *Phys. Rep.* **513** 1 (2012);
 S. Nojiri and S. D. Odintsov, *Int. J. Geom. Methods Mod. Phys.* **04** 115 (2007).
- [18] T. Faulkner, M. Tegmark, E. F. Bunn and Y. Mao, *Phys. Rev. D* **76**, 063505 (2007);
 S. Nojiri and S. D. Odintsov, *Int. J. Geom. Methods Mod. Phys.* **11**, 1460006 (2014);
 M. Cataneo et al., *Phys. Rev. D* **92**, 044009 (2015).
- [19] Yun-He Li and X. Zhang, *Phys. Rev. D* **89**, 083009 (2014);
 L. Amendola, *Phys. Rev. D* **62**, 043511 (2000);
 D. Comelli, M. Pietroni, and A. Riotto, *Phys. Lett. B* **571**, 115 (2003);
 X. Zhang, *Mod. Phys. Lett. A* **20**, 2575 (2005);
 R. G. Cai and A. Wang, *J. Cosmol. Astropart. Phys.* **03** 002 (2005);
 G. R. Farrar and P. J. E. Peebles, *ApJ* **604** (2004).

- [20] I. L. Shapiro, Phys. Rept. **357** 113 (2001) and references therein.
- [21] J. A. Helayel-Neto, A. Penna-Firme and I. L. Shapiro, Phys. Lett. **B 479** 411 (2000).
- [22] F. W. Hehl, P. von der Heyde, G. Kerlick and J. Nester, Rev. Mod. Phys. **48** 393 (1976);
 F. W. Hehl, J. D. McCrea, E. W. Mielke and Y. Ne'eman, Phys. Rept. **258** 1 (1995);
 F. W. Hehl and Y. N. Obukhov, Lect. Notes Phys. **562** 479 (2001).
- [23] V. de Sabbata and M. Gasperini, *Introduction to Gravitation*, World Scientific, Singapore (1985);
 V. de Sabbata and C. Sivaram, *Spin Torsion and Gravitation*, World Scientific, Singapore (1994).
- [24] A. K. Raychaudhuri, *Theoretical Cosmology*, Clarendon Press, Oxford (1979).
- [25] A. Trautman, Nature Phys. Sci. **242** 7 (1973).
- [26] R. T. Hammond, Gen. Rel. Grav. **23** 1195 (1991);
 R. T. Hammond, Gen. Rel. Grav. **32** 2007 (2000);
 R. T. Hammond, Rept. Prog. Phys. **65** 599 (2002).
- [27] P. Majumdar and S. SenGupta, Class. Quant. Grav. **16** L89 (1999).
- [28] A. Saa, Gen. Rel. Grav. **29** 205 (1996).
- [29] S. Kar, S. SenGupta and S. Sur, Phys. Rev. **D 67** 044005 (2003);
 S. SenGupta and S. Sur, Phys. Lett. **B 521** 350 (2001);
 S. SenGupta and S. Sur, JCAP 0312 001 (2003);
 S. SenGupta and S. Sur, Europhys. Lett. **65** 601 (2004);
 S. SenGupta and A. Sinha, Phys. Lett. **B 514** 109 (2001);
 D. Maity, S. SenGupta and S. Sur, Eur. Phys. J. **C 42** 453 (2005).
- [30] S. Kar, P. Majumdar, S. SenGupta and A. Sinha, Eur. Phys. J. **C 23** 357 (2002);
 S. Kar, P. Majumdar, S. SenGupta and S. Sur, Class. Quant. Grav. **19** 677 (2002);
 P. Das, P. Jain and S. Mukherji, Int. J. Mod. Phys. **A 16** 4011 (2001);
 D. Maity and S. SenGupta, Class. Quant. Grav. **21** 3379 (2004);
 G. F. Rubilar, Y. N. Obukhov and F. W. Hehl, Class. Quant. Grav. **20** L185-L192 (2003);
 D. Maity, S. SenGupta and S. Sur, Phys. Rev. **D 72** 066012 (2005);
 J. Alexandre, N. E. Mavromatos and D. Tanner, Phys. Rev. **D 78** 066001 (2008).
- [31] D. Maity, P. Majumdar and S. SenGupta, JCAP **0406** 005 (2004).

- [32] A. Chatterjee and P. Majumdar, Phys. Rev. **D 72** 066013 (2005);
S. Bhattacharjee and A. Chatterjee, Phys. Rev. **D 83** 106007 (2011).
- [33] B. Mukhopadhyaya, S. Sen and S. SenGupta, Phys. Rev. Lett. **89** 121101 (2002), Erratum-ibid. **89** 259902 (2002).
- [34] S. Sur, S. Das and S. SenGupta, JHEP **0510** 064 (2005);
T. Ghosh and S. SenGupta, Phys. Lett. **B 678** 112 (2009);
A. B. Balakin and W-T. Ni, Class. Quant. Grav. **27** 055003 (2010).
- [35] B. Mukhopadhyaya and S. SenGupta, Phys. Lett. **B 458** 8 (1999);
B. Mukhopadhyaya, S. SenGupta and S. Sur, Mod. Phys. Lett. **A 17** 43 (2002);
B. Mukhopadhyaya, S. Sen, S. SenGupta and S. Sur, Eur. Phys. J. **C 35** 129 (2004).
- [36] S. Capozziello, Mod. Phys. Lett. **A17** 1621 (2002);
S. Capozziello and S. Vignolo, Annalen Phys. **19** 238 (2010).
- [37] S. Capozziello, P.A. Gonzalez, E. N. Saridakis and Y. Vasquez, JHEP **1302** 039 (2013);
V. F. Cardone, N. Radicella and S. Camera, Phys. Rev. **D 85** 124007 (2012);
L. Iorio and E. N. Saridakis, Mon. Not. Roy. Astron. Soc. **427** 1555 (2012);
C. G. Böhrer, A. Mussa and N. Tamanini, Class. Quant. Grav. **28** 245020 (2011);
Y.-F. Cai, S.-H. Chen, J. B. Dent, S. Dutta and E. N. Saridakis, Class. Quant. Grav. **28** 215011 (2011);
B. Li, T. P. Sotiriou and J. D. Barrow, Phys. Rev. **D 83** 104017 (2011);
S. Capozziello, R. Cianci, C. Stornaiolo and S. Vignolo, Class. Quant. Grav. **24** 6417 (2007).
- [38] S. Capozziello and M. De Laurentis, Phys. Rept. **509** 167 (2011);
D. A. Carranza, S. Mendoza and L.A. Torres, Eur. Phys. J. **C73** no.1, 2282 (2013);
G. Allemandi *et al.*, Gen. Rel. Grav. **38** 33 (2006).
- [39] H.-J. Yo and J. M. Nester, Mod. Phys. Lett. **A 22** 2057 (2007);
J. M. Nester, L. L. So and T. Vargas, Phys. Rev. **D 78** 044035 (2008);
P. Baekler, F. W. Hehl and J. M. Nester, Phys. Rev. **D 83** 024001 (2011).
- [40] A. V. Minkevich, Phys. Lett. **B 678** 423 (2009);
A. V. Minkevich, A. S. Garkun and V. I. Kudin, Class. Quant. Grav. **24** 5835 (2007);
A. V. Minkevich, Phys. Lett. **A 80** 232 (1980).
K.-F. Shie, J. M. Nester and H.-J. Yo, Phys. Rev. **D 78** 023522 (2008);

- X.-Z. Li, C.-B. Sun and P. Xi, Phys. Rev. **D 79** 027301 (2009);
- X.-Z. Li, C.-B. Sun and P. Xi, JCAP **04** 015 (2009);
- H.-H. Tseng, C.-C. Lee, C.-Q. Geng, JCAP **1211** 013 (2012).
- [41] S. Sur, A.S. Bhatia, Class. Quant. Grav. **31** 025020 (2014).
- [42] M. Tsamparlis, Phys. Lett. **A 75** 27 (1979).
- [43] D. Gangopadhyay and S. SenGupta, *e-Print* arXiv: hep-th/9710139;
D. Gangopadhyay and S. SenGupta, *e-Print* arXiv: hep-th/9710138;
D. Gangopadhyay and S. SenGupta, *e-Print* arXiv: hep-th/9412238;
D. Gangopadhyay and S. SenGupta, Int. J. Mod. Phys. **A 14** 4953 (1999).
- [44] V. Faraoni, *Cosmology in Scalar-Tensor Gravity*, Kluwer Academic Publishers (2004).
- [45] V. Acquaviva *et al.*, Phys. Rev. **D 71** 104025 (2005);
A. Avilez and C. Skordis, Phys. Rev. Lett. **113** 011101 (2014);
X. Chen and F. Wu, Int. J. Mod. Phys. Conf. Ser. **01** 195 (2011).
- [46] J. Alsing *et al.*, Phys. Rev. **D 85** 064041 (2012).
- [47] S. Capozziello, G. Lambiase and C. Stornaiolo, Annalen Phys. **10** 713 (2001).
- [48] I. Bloomer, Gen. Rel. Grav. **9** 763 (1978).
- [49] V. A. Kosteleck, N. Russell and J. D. Tasson, Phys. Rev. Lett. **100** 111102 (2008).
- [50] Y. N. Obukhov, A. J. Silenko and O. V. Teryaev, Phys. Rev. **D90** 124068 (2014).
- [51] I. L. Buchbinder, S. D. Odintsov and I. L. Shapiro, Phys. Lett. **B162** 92 (1985);
I. L. Buchbinder and I.L. Shapiro, Izv. VUZov Fizika (Sov. J. Phys.) **31** (9) 40 (1988).
- [52] T. Jacobson and D. Mattingly, Phys. Rev. **D 64** 024028 (2001)
- [53] S. M. Carroll *et al.*, Phys. Rev. **D79** 065011 (2009);
S. M. Carroll *et al.*, Phys. Rev. **D79** 065012 (2009).
- [54] C. Gao *et al.*, Phys. Lett. **B702** 107 (2011).
- [55] S. Das *et al.*, The Atacama Cosmology Telescope: temperature and gravitational lensing power spectrum measurements from three seasons of data, J. Cosmology Astropart. Phys. **4** 14 (2014).
- [56] E. M. George *et al.*, A measurement of secondary cosmic microwave background anisotropies from the 2500-squared-degree SPT-SZ survey, arXiv:1408.3161

- [57] A. Conley *et al.*, Supernova Constraints and Systematic Uncertainties from the First Three Years of the Supernova Legacy Survey. *Astrophys. J. Suppl.* **192** 1 (2011)
- [58] C. Heymans *et al.*, CFHTLenS tomographic weak lensing cosmological parameter constraints: Mitigating the impact of intrinsic galaxy alignments, *MNRAS* **432** 2433 (2013).
- [59] A. J. Ross *et al.*, The Clustering of the SDSS DR7 Main Galaxy Sample I: A 4 per cent Distance Measure at $z=0.15$, arXiv:1409.3242;
P. McDonald *et al.*, *Astrophys. J. Suppl.* **163** 80 (2006).
- [60] M. Chevallier and D. Polarski, *Int. J. Mod. Phys.* **D10** 213 (2001);
E. V. Linder, *Phys. Rev. Lett.* **90** 091301 (2003).
- [61] See for e.g. E. Babichev, V. Mukhanov and A. Vikman, *JHEP* **0802** 101 (2008), and references therein.
- [62] S. del Campo, R. Herrera and P. Labrana, *JCAP* **0907** 006 (2009);
K. A. Bronnikov and S. G. Rubin, *Black Holes, Cosmology and Extra Dimensions*, World Scientific, Singapore (2013).
- [63] S. Sur and A. S. Bhatia, *Phase Plane Analysis of Dark Energy Models in Metric-Scalar-Torsion Theories*, in progress.
- [64] S. Sur *et al.*, *Effective LCDM via torsion-dust interactions*, in progress.